International Atomic Energy Agency

INDC(GDR)-39/L

INDC INTERNATIONAL NUCLEAR DATA COMMITTEE

DESCRIPTION OF FILE 8201 FOR LEAD FOR THE LIBRARY "BROND"

D. Hermsdorf
Technical University Dresden
Section of Physics

March 1986

IAEA NUCLEAR DATA SECTION, WAGRAMERSTRASSE 5, A-1400 VIENNA

Preface

File 8201 for natural Lead has been evaluated for the library BROND maintained at the Nuclear Data Centre (CJD) at FEI Obninsk.

The file has been specially designed for applications in fusion and hybrid reactor projects but also fulfils all data demands arising from thermal and fast reactor research.

The data have been evaluated in an international co-operation between TU Dresden and CJD Obninsk basing on independend investigations carried out in both institutions. This report compiles following individual contributions:

- T. Elfruth, D. Seeliger, K. Seidel, S. Unholzer
  "Double-differential neutron emission cross sections for Lead at 14 MeV"
  published in Proc. 13th Int. Symp. on Nuclear Physics, Gaussig, 1983, INDC(GDR)-34/GI, 1985
  to be published in Proc. Int. Symp. on Fast Neutron Physics, Chiang Mai, 1985 and
  in Proc. IVth Int. Symp. on Neutron-Induced Reactions, Smolenice, 1985
- D. Hermsdorf, H. Kalka, D. Seeliger, A.V. Ignatyuk, V.P. Lunev
  "Description of energy and angular distributions of fast neutron inelastic scattering by the Generalized Exciton Model"
  published in the Proceedings of the Conference on Neutron Physics, Kiev, 1983, Vol. I, p. 131
- D. Hermsdorf, H. Kalka, D. Seeliger
  "SMCR and SMDR in the frame of the Generalized Exciton Model"
  to be published in Proc. IVth Int. Symp. on Neutron-Induced Reactions, Smolenice, 1985
- V.P. Lunev
  "Calculation of direct reaction contributions to fast neutron inelastic scattering"
- A.I. Blokhin, A.V. Ignatyuk
  "Evaluation of resolved resonances parameters"

- D. Hermsdorf
  "Formatting of data according to new recommended rules of version V and VI of ENDF/B"
- D. Hermsdorf
  "Consistency checks of microscopic data for Lead by intercomparison with integral quantities"
  will be published in INDC(GDR)-report series separatly.

As usual, the file 8201 described here is under permanent development to include most recent results from nuclear reaction theory and experiments to meet more refined reactor application requirements.

This report documents the status of File 8201 at December 1985.

Contents

		Page
Preface		II
1.	General considerations	1
1.1.	Analysis of actual data demands	1
1.2.	Analysis of actual files of evaluated data and their relevance for customers needs	1
1.3.	General methods for evaluation of MAT 8201	3
1.4.	New experimental data base for MAT 8201	7
1.5.	Theoretical models applied for MAT 8201	8
2.	Comments on evaluated neutron nuclear data for MAT 8201	9
2.1.	Total cross section	9
2.2.	Elastic scattering cross section	13
2.2.1.	Integrated cross section	13
2.2.2.	Angular distributions for elastic scattered neutrons	18
2.3.	Neutron production cross section	24
2.3.1.	Neutron inelastic scattering cross section	26
2.3.1.1.	Excitation of discrete levels	26
2.3.1.2.	Excitation of level continuum	29
2.3.1.3.	Angular distribution of primary emitted neutrons	34
2.3.1.4.	Total neutron inelastic scattering cross section	38
2.3.2.	(n,2n) cross sections and secondary neutron emission spectra	40
2.3.3:	(n,3n) reaction cross sections	47
2.3.4.	Further neutron emitting reaction cross sections	47
2.3.5.	Neutron-induced fission cross sections	51
2.4.	Neutron absorption reactions	51
2.4.1.	Neutron capture cross sections	51
2.4.2.	Charged particle production cross sections	55
2.4.2.1.	Proton emission cross sections	55
2.4.2.2.	Alpha-particle emission cross sections	57
2.4.2.3.	Deuteron-emission cross sections	57
2.4.2.4.	Triton-emission cross sections	59
2.5.	Non-elastic cross sections	59
2.6.	Parameters for resolved resonances	60

		Page
3.	Neutron-induced γ-ray emission cross sections	68
3.1.	γ-ray production cross sections	68
3.2.	γ-ray angular distributions	68
3.3.	γ-ray spectra	71
4.	Representation of uncertainties in ENDF/B-format (MF33)	71
5.	Summary remarks	73
List of references		75

1. General considerations

1.1. Analysis of actual data demands

Analysing recent data requests for Lead compiled in the last and preceding issues of WRENDA /1,2,3/ mainly two data types appear of high interest:

i) energy-angle dependence of fast neutron inelastic scattering and
ii) energy-angle dependence of neutron-induced production of γ-quanta and charged particles.

The importance results from the fact that Lead is one of the prefered candidates of fusion or hybrid reactor materials for neutron multiplier. So, the investigation of neutron production and radiation damage effects are of highest priority.

Table 1 summarizes data requests for Lead taken from /1,2,3/.

The appearance of any data request in WRENDA means that our present day knowledge concerning experimentally proofed informations are insufficient in both accuracy achieved and measuring technique applied.

However, also most qualified and developed evaluated data files only reflect these deficiencies.

1.2. Analysis of actual files of evaluated data and their relevance for customers needs

All files for Lead actual and available from NDS of IAEA are compiled in table 2.

The contents of each file depends strongly on the data demands requested for as well as data library and the special file. A review of evaluated data quantities given in several files is given in table 3.

Table 1: Compilation of data requests for Lead (taken from WRENDA-lists /1,2,3/).

Quantity	79/80 /1/		81/82 /2/		83/84 /3/	
	energy range (in MeV)	accuracy (in %)	energy range (in MeV)	accuracy (in %)	energy range (in MeV)	accuracy (in %)
(n,n')	3-5	15	-	-	3-15	15
(n,2n)	0-15	15	0-15	10-20	0-15	10-15
(n,3n)	-	-	5-15	20	14-15	20
n-production	0.5-16	5-10	2-16	5-10	0.5-16	5-10
p-production	14	-	-	-	-	-
α-production	14	-	-	-	0-15	20
(n,γ)	-	-	0.002-0.6	5	0.002-0.6	5
γ-ray production	0-16	10-15	-	-	0-16	10-15

Comparing recent data requests and the available corresponding (and relevant) evaluated quantities, generally energy-angle-dependent cross sections (DDX) for neutron and charged-particle production are missing (MF6). First attempts have been done for the CJD library BROND (this file MAT 8201) and for the libraries JEF-2 and EFF-2 /4/.

Furthermore, data for γ-production required for combined neutron-γ-quanta transport calculations are missing generally too.

Some of the data types (the standard ones) are included in all libraries. But this doesn't ensure a priori a reasonable agreement between results of different evaluations. Such deviations arise from an inconsistent and insufficient experimental data base available and processed in the evaluation task.

To create this file MAT 8201 these discrepancies had been investigated especially very carefully by means of most recent experimental values and theoretical studies.

Unfortunatly, up to now evaluated data are given without error quotes. Therefore, in MAT 8201 estimated uncertainties for all integrated data types (MT1,2,4,10,16,17,91,102,103 and 107) are compiled and formatted according to MF33 rules of ENDF/B.

1.3. General methods for evaluation of MAT 8201

All files for Lead available and commonly used have been evaluated on the basis of experimental data published up to 1973/74 at least (compare table 2).

Therefore, the evaluation of file 8201 has been guided by four principles:

i) starting-point for each quantity was the corresponding data type of the most recent and developed file MAT 1288 of the ENDF/B-IV library.

ii) all experimental data obtained later than 1974 have been carefully inspected according to their relevance for updating and improving of corresponding MT's in MAT 1288.

Table 2: Files of evaluated nuclear data for Lead.

Library	Accession number	Isotope	Date of evaluation	Format
ENDF/B-IV	MAT 1288	natural	1971 revision 1974	ENDF/B version IV
JENDL-2	MAT 2820 MAT 2821 MAT 2822 MAT 2823 MAT 2824	natural 204-Pb 206-Pb 207-Pb 208-Pb	1981 revision 1984	ENDF/B version IV
UKNDL-80	DFN 26C	natural	unknown (~1975)	UKNDL
ENDL-82 ENDL-84	ZA 82000	natural	~1978 (data identi- cal with ENDL-78) identical to ENDL-82	ENDL transmittal format, available in ENDF/B version V in ENDL-84 ENDF/B-V
INDL/V	MAT 8230 MAT 8240	204-Pb 208-Pb	1980	ENDF/B version IV
BROND (CJD)	MAT 8201	natural	1985	ENDF/B version V and IV (partially)

Table 3: Data types evaluated for several libraries (MF's and MT's according to ENDF/B momenclature).

MT	MF2		MF3						MF4					MF5				
	1)	2)	1)	2)	3)	4)	5)	6)	1)	2)	3)	5)	6)	1)	2)	3)	5)	6)
1	-	-	x	x	x	-	x	x	-	-	-	-	-	-	-	-	-	-
2	-	-	x	x	x	-	x	x	x	x	x	x	x	-	-	-	-	-
3	-	-	x	-	x	-	-	x	-	-	-	-	-	-	-	-	-	-
4	-	-	x	x	x	-	x	x	-	-	-	-	-	-	-	-	-	-
10*	-	-	x	-	-	-	-	-	-	-	-	-	-	x	-	-	-	-
16	-	-	x	x	x	x	x	x	-	-	-	-	-	x	x	x	x	x
17	-	-	x	x	x	-	x	-	-	-	-	-	-	x	x	x	x	-
22	-	-	x	x	-	-	-	-	-	-	-	-	-	-	x	-	-	-
28	-	-	x	x	-	-	-	-	-	-	-	-	-	-	x	-	-	-
51-90	-	-	-	x	x	-	-	-	-	-	x	-	-	-	-	-	-	-
91	-	-	x	x	x	-	x	-	-	-	-	-	-	x	x	x	x	x
101	-	-	x	-	-	-	-	-	-	-	-	-	-	-	-	-	-	-
102	-	-	x	x	x	-	x	x	-	-	-	-	-	-	-	-	-	-
103	-	-	x	x	-	-	-	-	-	-	-	-	-	-	-	-	-	-
107	-	-	x	x	-	-	-	-	-	-	-	-	-	-	-	-	-	-
151	x	x	-	-	-	-	-	-	-	-	-	-	-	-	-	-	-	-
251	-	-	x	x	x	-	x	-	-	-	-	-	-	-	-	-	-	-
252	-	-	x	-	x	-	x	-	-	-	-	-	-	-	-	-	-	-
253	-	-	x	-	x	-	x	-	-	-	-	-	-	-	-	-	-	-
719	-	-	x	-	-	-	-	-	-	-	-	-	-	x	-	-	-	-
799	-	-	x	-	-	-	-	-	-	-	-	-	-	x	-	-	-	-

Footnotes:

* MT10 according to lumped cross section for neutron production

1) this file, MAT 8201

2) JENDL-2, MAT 2820

3) ENDF/B-IV, MAT 1288

4) INDL/V, MAT 8230 and MAT 8240

5) ENDL-82, ZA 82000

6) UKNDL, DFN 26C

Table 3: contn'd

MT	MF6	MF12			MF13			MF14			MF15			MF33
	1)	1)	3)	5)	1)	3)	5)	1)	3)	5)	1)	3)	5)	1)
1	-	-	-	-	-	-	-	-	-	-	-	-	-	x
2	-	-	-	-	-	-	-	-	-	-	-	-	-	x
3	-	-	x	-	x	-	x	-	x	-	x	x	x	-
4	-	-	-	-	-	-	-	-	-	-	-	-	-	x
10*	x	-	-	-	-	-	-	-	-	-	-	-	-	x
16	-	-	-	-	-	-	-	-	-	-	-	-	-	x
17	-	-	-	-	-	-	-	-	-	-	-	-	-	x
22	-	-	-	-	-	-	-	-	-	-	-	-	-	-
28	-	-	-	-	-	-	-	-	-	-	-	-	-	-
51-90	-	-	-	-	-	-	-	-	-	-	-	-	-	-
91	-	-	-	-	-	-	-	-	-	-	-	-	-	x
101	-	-	-	-	-	-	-	-	-	-	-	-	-	-
102	-	x	-	x	-	-	-	x	-	x	x	-	x	x
103	-	-	-	-	-	-	-	-	-	-	-	-	-	x
107	-	-	-	-	-	-	-	-	-	-	-	-	-	x
151	-	-	-	-	-	-	-	-	-	-	-	-	-	-
251	-	-	-	-	-	-	-	-	-	-	-	-	-	-
252	-	-	-	-	-	-	-	-	-	-	-	-	-	-
253	-	-	-	-	-	-	-	-	-	-	-	-	-	-
719	-	-	-	-	-	-	-	-	-	-	-	-	-	-
799	-	-	-	-	-	-	-	-	-	-	-	-	-	-

iii) strong discrepancies resulting from an intercomparison between corresponding MT's in all libraries have been especially investigated by use of new experiments and model calculations.

iv) new data quantities required for MAT 8201 have been evaluated on the basis of both experimentally and theoretically obtained and verified results.

It should be noticed that the evaluation of MAT 8201 has been done simultaneously with but totally independend on evaluation efforts for JENDL-2. Therefore, comparison of results for the same quantity obtained by both evaluations reflects to some extend the accuracy achieved at presentas well as in measuring technique and theoretical models calculations.

1.4. New experimental data base for MAT 8201

Since 1974 extensive and systematical studies of fast neutron elastic and inelastic scattering for ^{208}Pb and ^{nat}Pb have been carried out by use of highly refined measuring techniques as well as in energy and angular resolution.

New results have been obtained for:

i) elastic scattering on ^{208}Pb in the range from 4 to 26 MeV by the Ohio State University group /5,6/ resulting in an improved set of global optical model potential parameters.

ii) inelastic scattering on ^{208}Pb in the range from 7 to 26 MeV by the Ohio State University group /7,8/ too yielding informations on the collective nature of low-lying levels in ^{208}Pb (nuclear deformation parameters) in dependence on the incidence energy.

iii) double-differential cross sections for fast neutron inelastic scattering on ^{nat}Pb at 14 MeV by the TU Dresden group /10/ and the Osaka University group /11/ with improved accuracy and energy resolution in comparison to past experiments carried out by TU Dresden /9/ and the California University formerly /12/.

iv) the (n,2n) excitation function by Frehaut et al. /13/.

All these new data gave rise to supersede older data constituting a new data base for evaluation in the time being.

1.5. Theoretical models applied for MAT 8201

For calculations in terms of nuclear reaction mechanisms some well-known but also recently developed models have been applied. Standard calculations with the Optical Model and the Hauser-Feshbach-Formalism were performed by means of the computer codes ELIESA /14/ and STAPRE /15/. To estimate reaction contributions to neutron inelastic scattering different models and corresponding computer codes were used:

i) the enhancement of excitation strength of low-lying levels due to collective effects in neutron inelastic scattering on ^{208}Pb has been calculated using DWBA and CC model codes /16/.

ii) the angular dependence of neutron inelastic scattering to the level continuum has been estimated in terms of the "Leading-Particle-Model" implemented in the code AMAPRE /17/.

iii) non-equilibrium effects in neutron emission spectra have been calculated in the frame of the Generalized Exciton Model using the code AMAPRE too.

iv) direct contributions to γ-ray production in neutron capture have been provided for by codes FISPRO /18/ and PEQGM /19/ which rely upon the Direct-Semidirect-Model and the Exciton Model for γ-quanta respectively.

Only such an arsenal of different partially contrary but, nevertheless, supplementary models (and the corresponding computer codes) deliver a consistent and complex interpretation of the experimental data base and ensures the prediction of unmeasured data within an accuracy of reasonable confidence.

2. Comments on evaluated neutron nuclear data for MAT 8201

2.1. Total cross section

The total cross section in MAT 8201 is given in two energy ranges:

- from 10^{-5} eV to 1.6 MeV by resolved resonances parameters evaluated by A.V. Blokhin /20/;
- from 1.6 MeV to 20 MeV in a point-wise representation basing on experimental data by Schwartz /21/.

In fig. 1 the total cross section in the fast neutron energy region is represented and compared to data given in other libraries.

The uncertainties of data have been estimated to be

up to	5 %	from 10^{-5} eV to 1 MeV
	1 - 5 %	from 1 MeV to 15 MeV
and	1 %	up to 20 MeV

in accordance with experimental error bands. In comparison to other measured cross sections the total cross section is the most precise quantity. Generally, σ_{nT} is used for adjustment of other experimentally or theoretically determined cross sections. The predictive power of theoretical methods (Optical Model) with different parameter sets is in the same order of accuracy (2-5 %) unless generalized parameter sets (for mass and/or energy ranges) are used.

Then the uncertainty of calculated total cross sections varies from 10 to 5 % with increasing energy (see fig. 2).

A special study has been carried out at 10 MeV by comparing results obtained with best-fit parameters, generalized potentials for Lead /5,6,7,8,22,23,24,25/ and the global optical potential by Becchetti-Greenless /26/. All the data are reviewed in table 4.

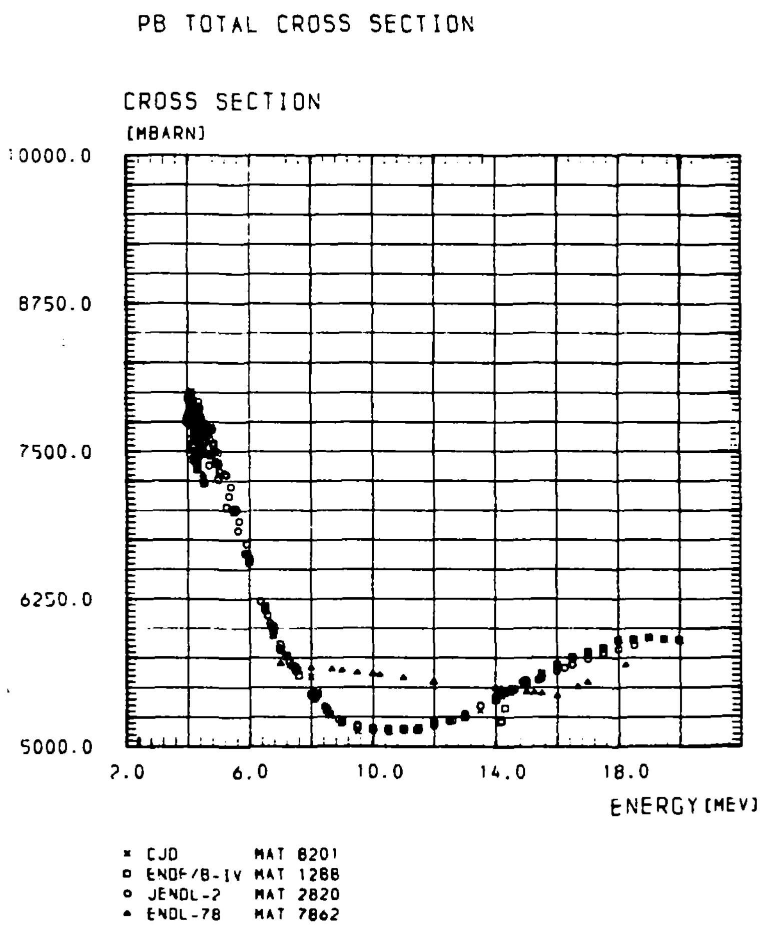

Fig. 1: Total cross section for natural Lead.
Data given in several evaluated nuclear data libraries are intercompared.

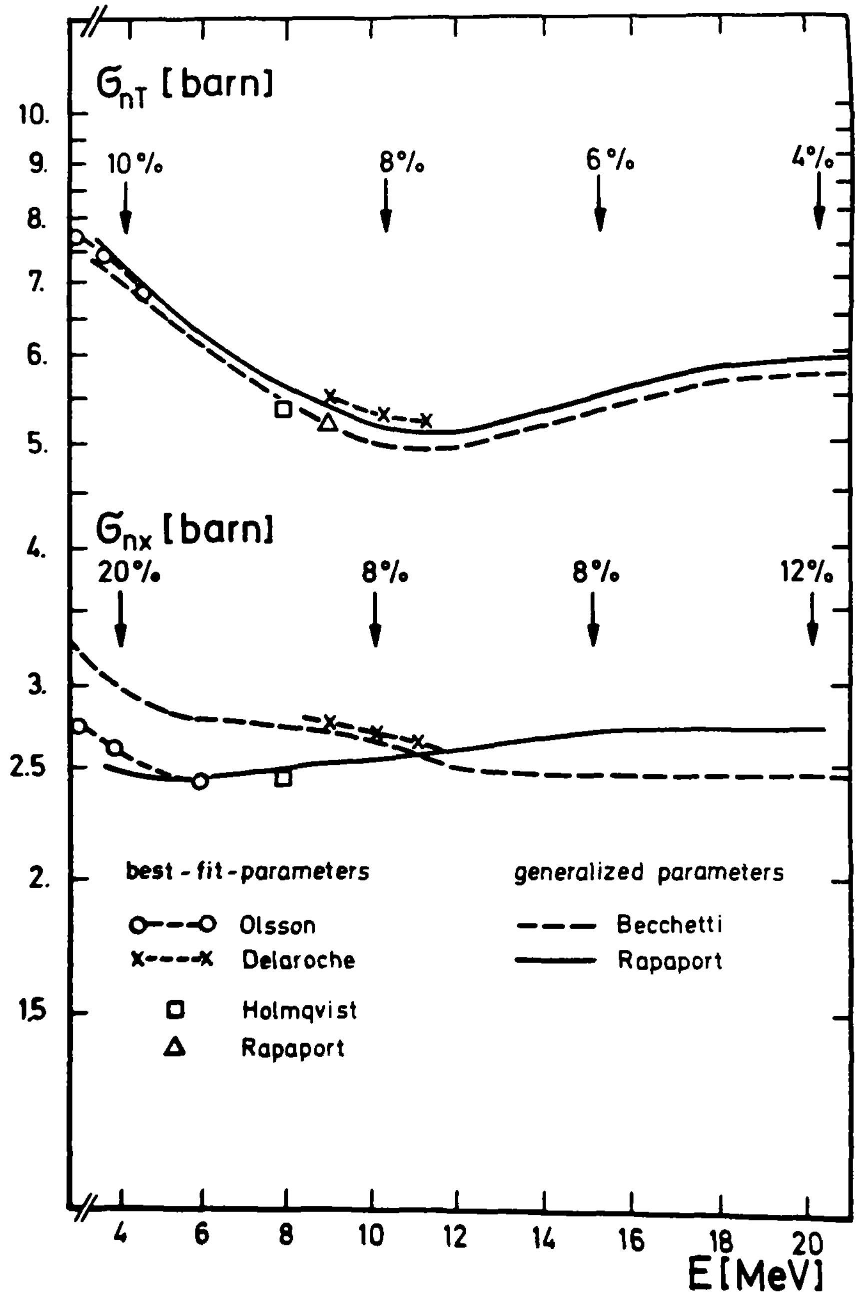

Fig. 2: Total and non-elastic cross sections calculated by the Optical Model using various parameter sets. Overall deviations between results of different parameter sets are given. Optical parameter sets have been taken from Olsson et al. /24/, Delaroche et al. /23/, Holmqvist et al. /25/, Rapaport et al. /8/ and Becchetti et al. /26/.

Table 4: Total cross sections (in barns) predicted by best-fit and generalized optical potentials.

Potentials	Reference	Energy/MeV					
		7	8.05	9	10	11	12
best-fit parameters	/7/	5.82	-	5.28	-	5.33	-
	/23/	-	-	-	5.25	-	-
	/25/	-	5.39	-	-	-	-
	/65/	5.81	-	5.27	5.31	-	-
generalized for A=208	/5/	5.98	5.57	5.32	5.18	-	5.17
	/6/	5.86	5.45	5.23	5.13	5.10	5.13
	/7/	5.94	-	5.21	-	5.08	-
	/24/	5.83	5.54	5.30	5.12	5.01	-
	/25/	5.65	5.29	5.17	4.99	4.88	-
global potential	/26/	-	5.44	-	5.01	-	5.01
Experimental values	/7/	5.85	-	5.21	-	5.22	-
	/25/	-	5.42 $\pm$0.1	-	-	-	-

2.2. Elastic scattering cross section

2.2.1. Integrated cross section

Commonly the angle-integrated elastic scattering cross section is derived by subtracting the non-elastic cross section from the total one. This method may be legal as long as both the experimental accuracy and the theoretical models produce elastic scattering and partial reaction cross sections with inadequate precision.

For evaluation of elastic scattering cross sections for MAT 8201 this method was practised too. However, the cross sections obtained have been tested very carefully by Optical Model calculations. Different types of potentials as well as best-fit parameter sets extracted for single energy points /7,23,25/, generalized over an energy range for A = 206 or 208 /5,6,7,24,25/ and a global potential /26/ have been applied in calculations to estimate the accuracy achievable.

At present, the uncertainty of measured fast neutron elastic scattering cross section is not better than 4 - 10 % resulting from inherent errors in experimental techniques (TOF-method usually) and numerical data processing procedures additionally /27/. Of course, any best-fit parameter set can reproduce the experimental data within the same or something enlarged (up to 20 - 30 %) uncertainty.

Therefore, elastic cross sections estimated by generalized optical potentials don't deviate stronger from individually determined values (compare table 5 and fig. 3).

Analogous investigations for the low energy region ($E < 3$ MeV) have to take into account considerable contributions from compound-elastic processes. All results strongly depend on the number of reaction channels for non-elastic processes (open channels) included in the calculations (compare table 6).

At lower energies (< 1 MeV) the elastic cross section shows strongly fluctuating structures hardly to be interpreted in terms of theoretical models as well as in resolved-resonances analysis.

Table 5: Elastic scattering cross sections (in barns) predicted by best-fit, generalized and global potential parameter sets.

Potential	Reference	Energy/MeV 7	8.05	9	10	11	12
best-fit potential	/23/	-	-	-	2.59	-	-
	/24/	3.14	-	-	-	-	-
	/25/	-	2.95	-	-	-	-
	/65/	3.42	-	2.68	2.60	-	-
generalized parameters for A=206, 208	/5/	3.47	3.02	2.74	2.59	-	2.57
	/6/	3.37	2.92	2.66	2.53	2.52	2.58
	/24/	3.13	2.85	2.66	2.55	2.50	-
	/25/	3.15	2.83	2.73	2.66	2.63	-
global potential	/26/	-	2.63	-	2.33	-	2.42
Experimental value	/24/	2.75 $\pm$0.11	-	-	-	-	-
	/25/	-	2.20 $\pm$0.13	-	-	-	-
	/6,65/	3.30	-	-	-	-	-

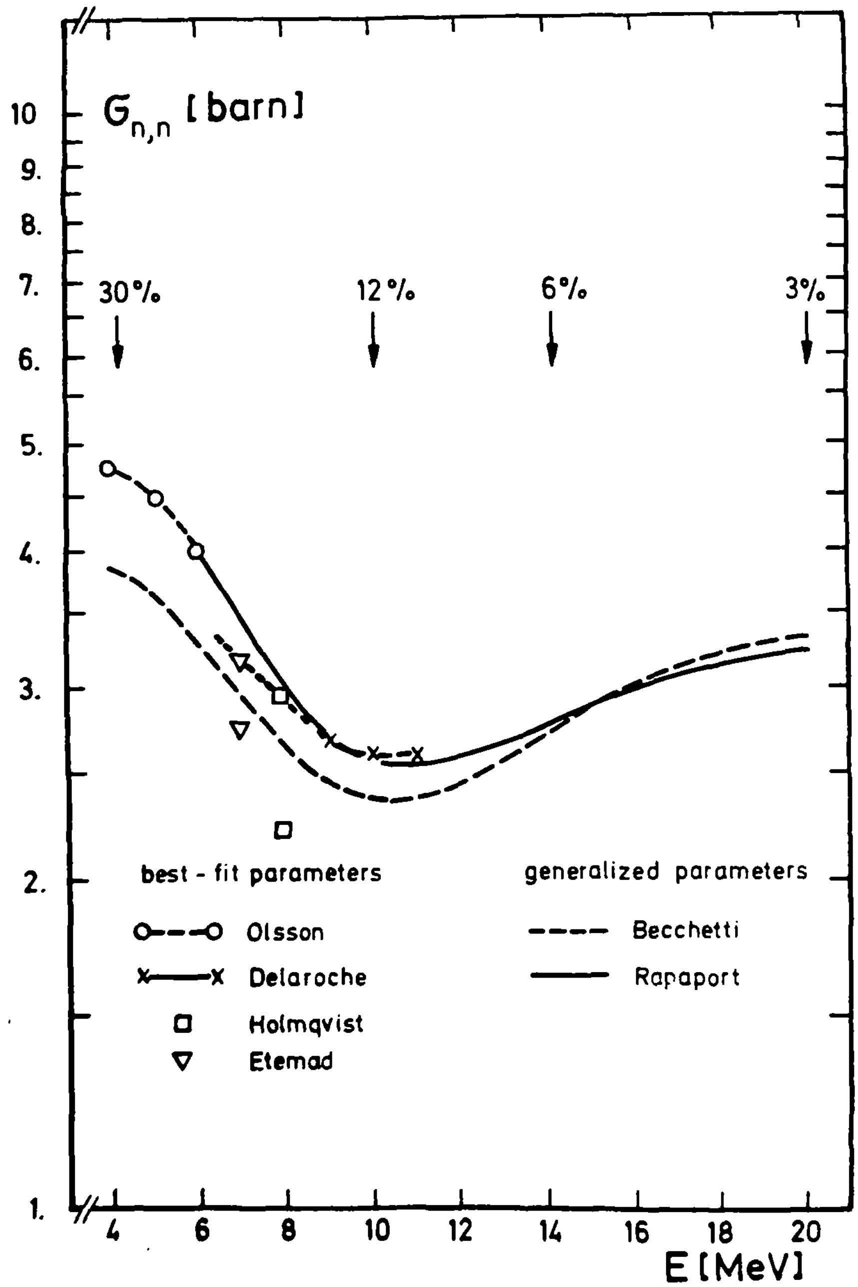

Fig. 3: Elastic scattering cross section calculated by various optical potentials. Overall deviations between different parameter sets are shown.
Parameter sets have been taken from Olsson et al. /22/, Delaroche et al. /23/, Holmqvist et al. /25/, Etemad /24/, Rapaport et al. /8/ and Becchetti et al. /26/.

Table 6: Elastic scattering cross sections (in barns) predicted by Optical and Statistical Model analysis.

Energy E/MeV	Scattering cross sections shape elastic (SOM)*		compound elastic (H-F)**		(H-F)***
1.485	3.336	/22/	1.0	/22/	0.65
2.975	4.82	/22/	0.4	/22/	0.164
3.975	4.786	/22/	0.2	/22/	0.0756
	5.2	/6,65/	1.2	/6,65/	

* Spherical Optical Model (SOM) parameters.

** only ground-state transition calculated.

*** up to 30 discrete levels in the residual nucleus considered (code ELIESA /14/).

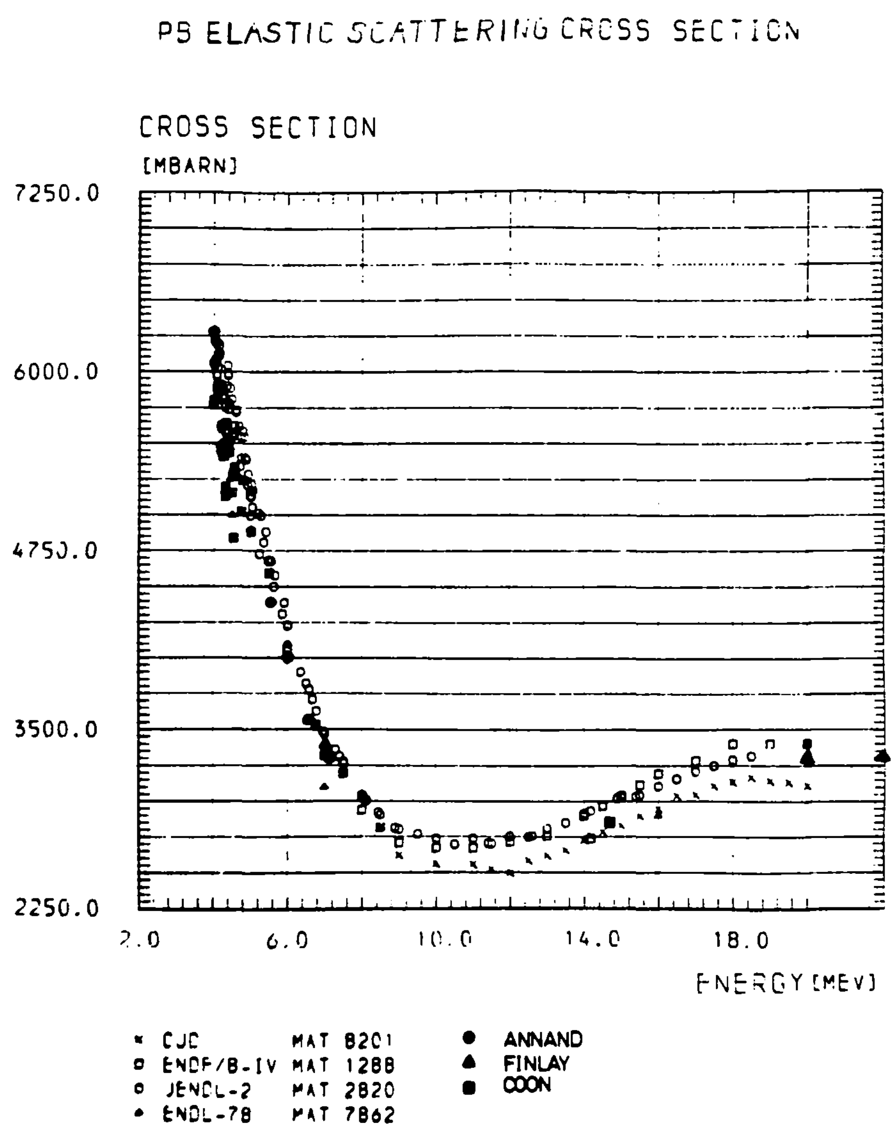

Fig. 4: Elastic scattering cross section given in several nuclear data libraries.

Nevertheless, in MAT 8201 the elastic scattering cross section is given in two ranges:

i) from 10^{-5} eV to 1.6 MeV in terms of Multi-Level-Breit-Wigner resonances parameters /20/ (MLBW);

ii) from 1.6 to 20 MeV in point-wise representation.

Estimated error quotes given in MF33 are derived from uncertainties in σ_{nT} and σ_{nX} correspondingly.

Figure 4 demonstrates a comparison of elastic scattering cross sections in the fast neutron region recommended in several libraries.

2.2.2. Angular distributions for elastic scattered neutrons

The representation of angular distributions in terms of normalized coefficients f_l of a Legendre-polynomial expansion seems very advantageous because of a more or less independence (insensitivity) to uncertainties in the integral cross section.

However, these coefficients are known to a relatively limited level of confidence too by experimental uncertainties or Optical Model predicting deficiencies.

Two coefficients f_l for orbital momenta $l = 1$ and 3 respectively are given in figs. 5 and 6 to show experimental accuracies achieved at present and to illustrate deviations resulting from different optical potentials. Generally, the spread in calculated data are lower than the experimental uncertainties reported in the original papers.

Especially, diverging results for all coefficients f_l at energies above 10 MeV should be investigated experimentally in the future.

It is quite difficult to draw definite conclusions from quoted errors in f_l on the uncertainties in the corresponding angular distribution because of correlations between all coefficients /27/. Therefore, the complete covariance matrices have to be stored in MF34 which is proposed for inclusion in ENDF/B /28/.

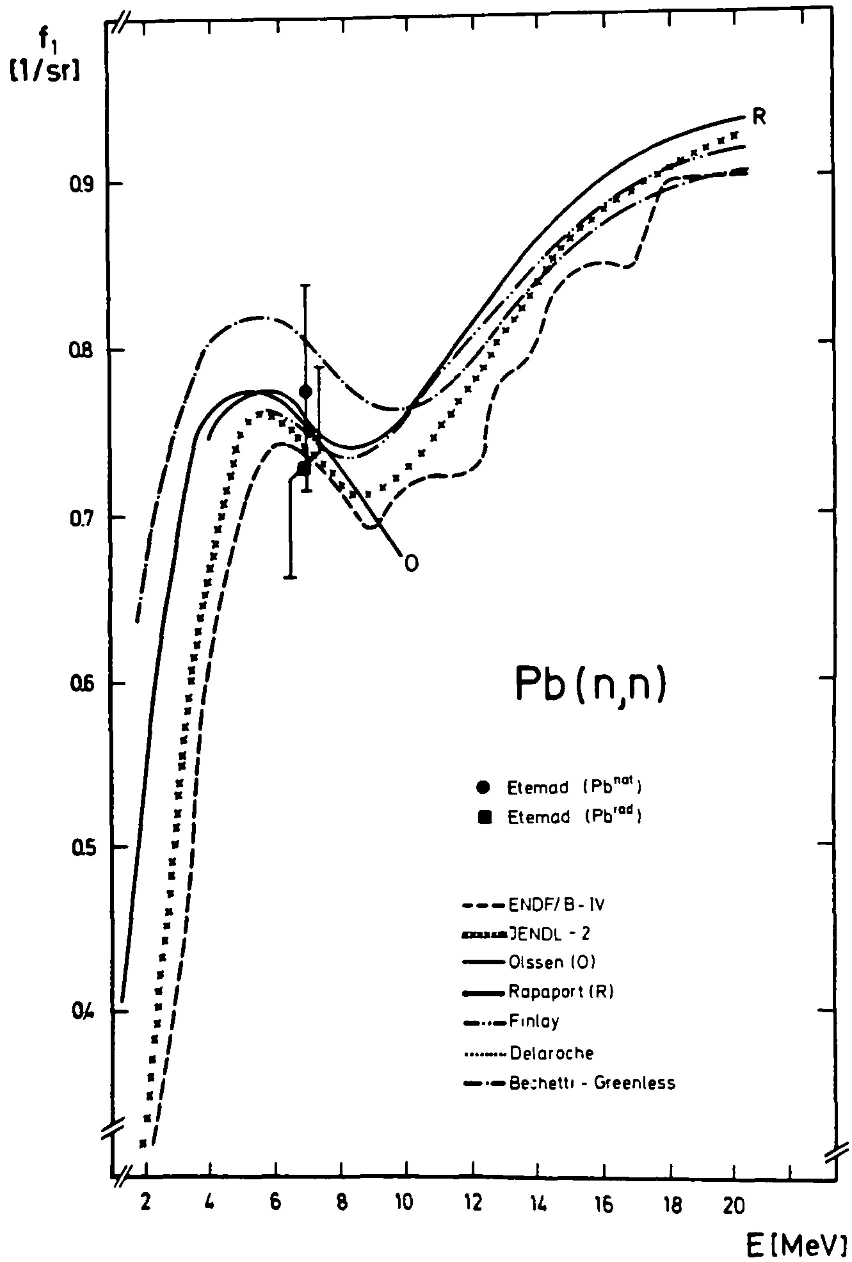

Fig. 5: First-order Legendre polynomial coefficient f_1 for elastic scattering.
Different lines corresponds to various optical potential parameter sets taken from refs. /6,8,22,23,26/. Coefficients derived from measurements on ^{nat}Pb and ^{rad}Pb (radiogenic Lead; A ≈ 206) by Etemad /24/ demonstrate the experimental accuracy.

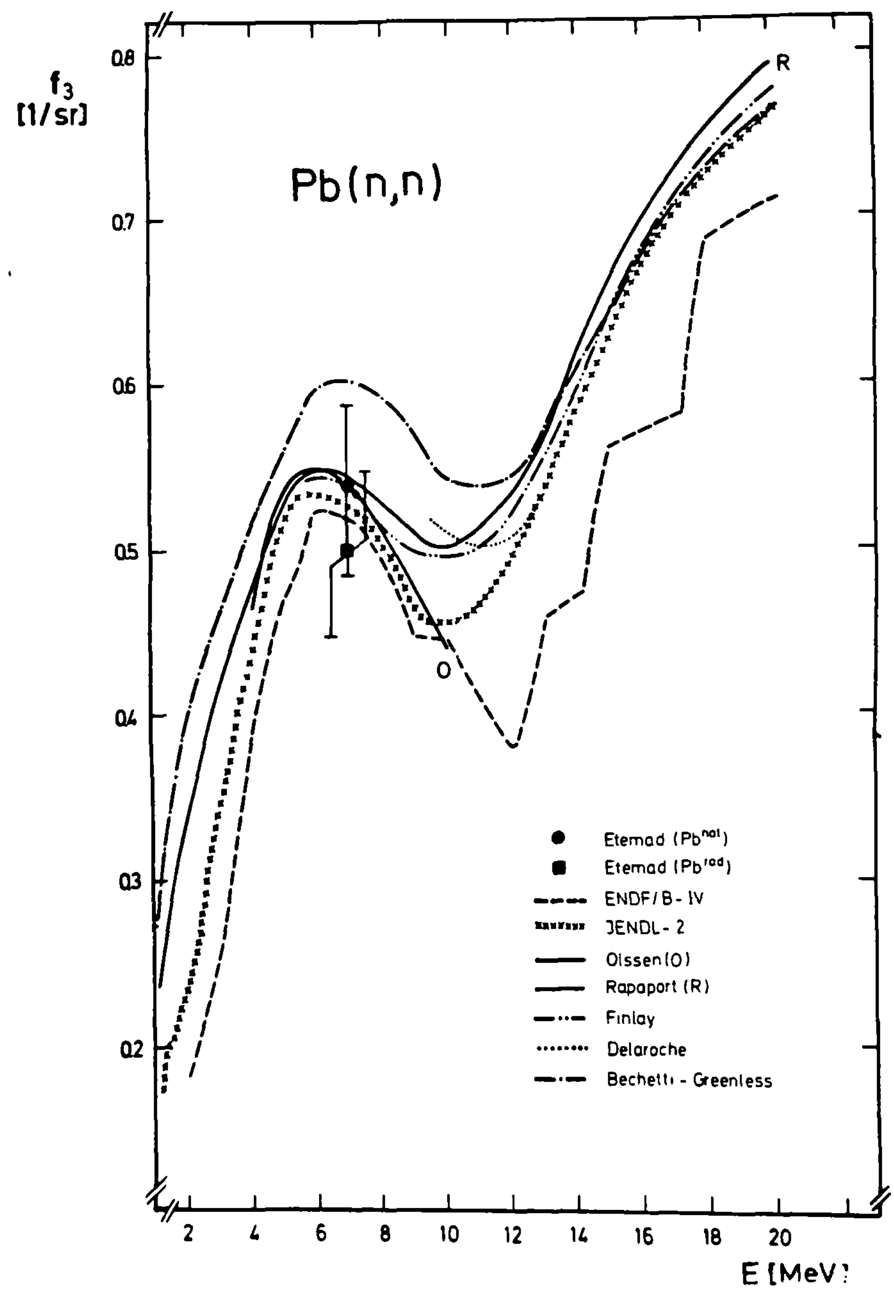

Fig. 6: Third-order Legendre polynomial coefficient f_3 for elastic scattering.
(For further details see caption to fig. 5.)

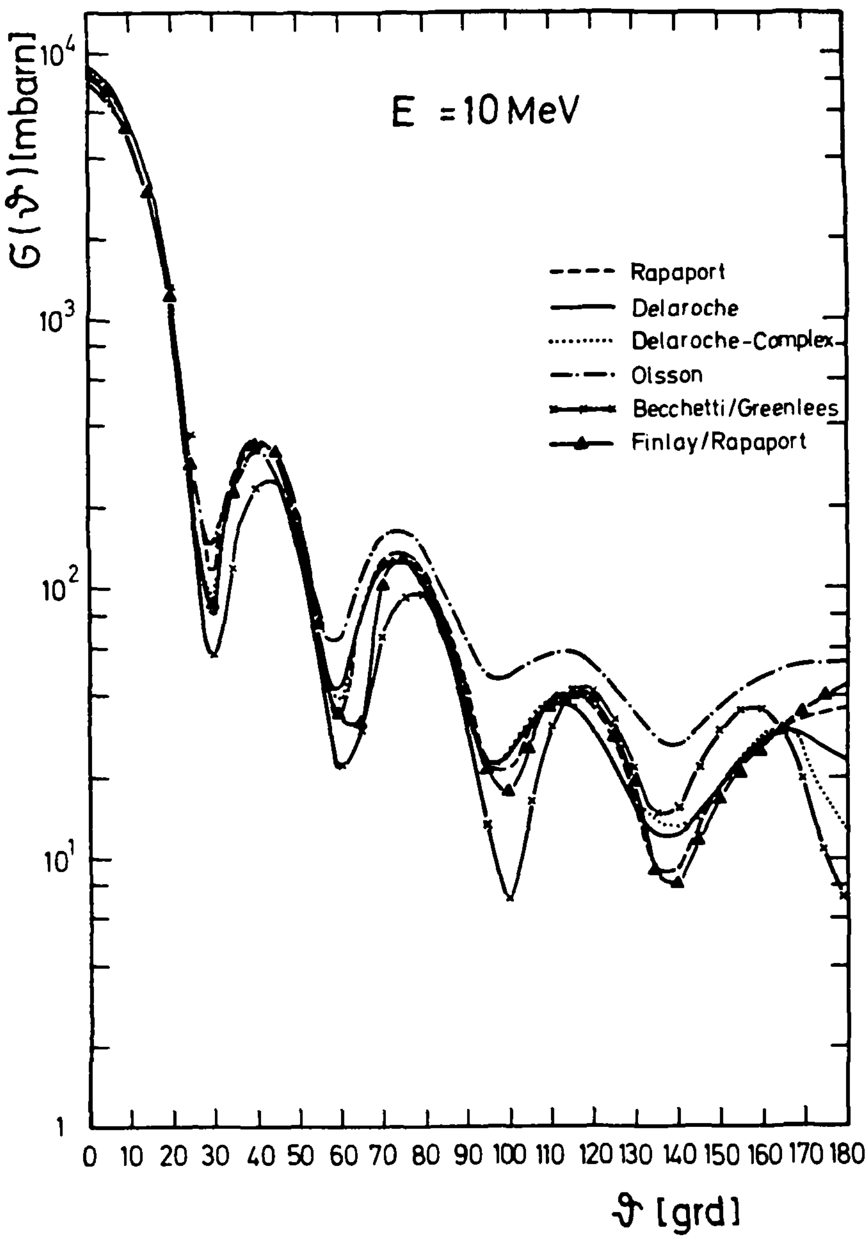

Fig. 7: Angular distribution of elastic scattering of 10 MeV neutrons.
Different Optical Model calculations are intercompared. Parameter sets have been taken from Rapaport et al. /5/, Delaroche et al. /23/, Olsson et al. /22/, Finlay et al. /6/ and Becchetti et al. /26/.

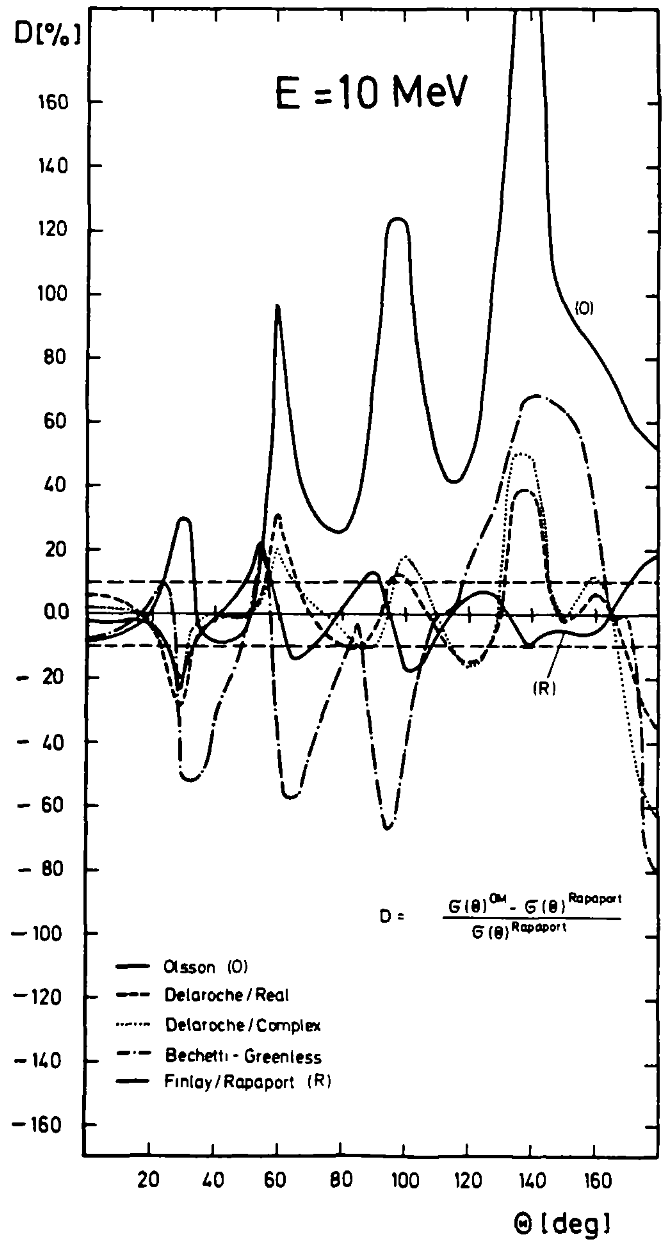

Fig. 8: Deviations of different Optical Model predictions for neutron elastic scattering relativ to Rapaports potential /5,6/ at 10 MeV.
The very strong deviations of Olsson's predictions /22/ demonstrate the inadmissible extrapolation of the corresponding potential to energies higher than 4 - 5 MeV. Furthermore, parameter sets valid at 10 MeV have been taken from Delaroche et al. /23/ and Becchetti et al. /26/.

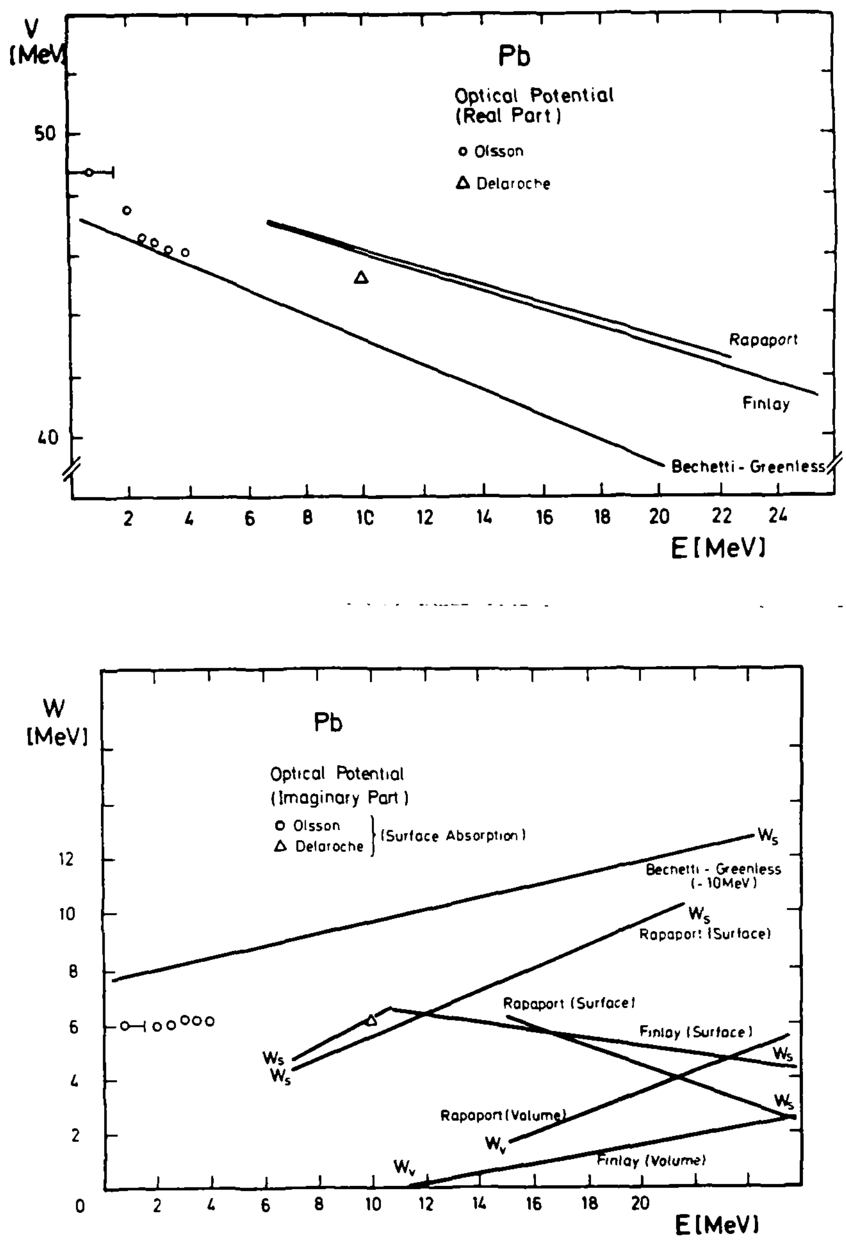

Fig. 9: Optical potential depths for the real (V) and imaginary (W) part extracted and proposed by different elastic scattering analysis.
Parameter sets have been taken from Olsson et al. /22/, Delaroche et al. /23/, Rapaport et al. /5/, Finlay et al. /6/ and Becchetti et al. /26/.

Real discrepancies in an angular distribution predicted by different Optical Model calculations are shown in fig. 7. They are varying from a few percent up to an order of magnitude in the vicinity of minima and maxima in pronounced structured angular distributions above 10 MeV (fig. 8). For MAT 8201 the coefficients f_l have been calculated on the basis of Rapaports' generalized potential /5,6/. The corresponding parameters for potential strenghts are shown in fig. 9.

2.3. Neutron production cross section

The cross section for neutron production σ_{nM} is a lumped quantity summarizing all cross sections of non-elastic processes resulting in neutron emission.

For the version ENDF/B-VI a new data type MT10 has been proposed /28/ for representation of such data. For MAT 8201 a slightly modified sum rule has been applied

$$\begin{aligned} MT10 = {} & MT4 + MT16 + MT17 + MT22 + MT28 + MT103 + MT104 \\ & + MT105 + MT106 + MT107 + MT719 + MT799 \end{aligned}$$

and

$$MT4 = MT51 \ldots MT90 + MT91.$$

Then σ_{nM} is obtained from MT10 by the relation

$$\sigma_{nM} = \nu \cdot MT10$$

introducing a neutron multiplication factor ν and

$$\nu = \sigma_{nM}/(\sigma_{nX} - \sigma_{abs}) .$$

This procedure is in accordance with proposed rules for MF6 of ENDF/B-VI too /28/. Neutron production cross sections have been investigated experimentally at 14 MeV only.

Table 7: Fractions of energy ranges in the neutron emission spectrum to the total neutron production cross section σ_{nM}.

Author	Energy range (in MeV)				σ_{nM}
	0-2.	2.-6.4	6.4- 14.	2.- 14.	(in mbarn)
Hermsdorf et al. /9/	2410 *	1513	434	1930 ±200	4340 ±440
Elfruth et al. /10/	-	2427	339	2766	-
Takahashi et al. /11/	2689 **	1751	343	2094	4783
Yanagi et al. /35/	3109 ***	-	-	-	5000 ±300 ***
Kammerdiener /12/	-	-	-	1975 ±200	-
Schectman ****	-	1600 ±330	-	-	-

* estimated by semi-empirical model described in D. Hermsdorf et al., Kernenergie 16 (1973) 252

** integrated in the energy range 0.7 to 2 MeV only

*** calculated from the measured quantity (4660±250) mbarn in the range 0.08 to 6.4 MeV using complementary values from Takahashi et al. /11/

**** according to R.M. Schectman, J.D. Anderson, Nucl. Phys. 77 (1966) 241; the measured value at 90^{o} have been multiplied by 4π assuming isotropic angular distributions

Table 7 summarizes the results obtained from several measurements of the neutron emission spectrum at 14 MeV. Comparing different ranges of emission energy then the most crucial fraction contributing dominantly to the neutron production cross section σ_{nM} comes from the range 0 to 2 MeV. But, this energy region is quite difficult to analyse in TOF-experiments. Therefore this fraction is determined as well as experimentally and theoretically with moderate accuracy only.

However, the total neutron production cross section σ_{nM} is known to an accuracy of about 10 % to be (4800±500) mbarn only. Such a large uncertainty can't remove principally discrepancies coming from uncertain knowledge of elastic and non-elastic cross sections (see chapter 2.5.).

2.3.1. Neutron inelastic scattering cross section

2.3.1.1. Excitation of discrete levels

Natural Lead is composed of four isotopes with non-vanishing abundances resulting in a quite complex spectrum of low-lying levels.

At an excitation energy of 4.3 MeV a total of 90 discrete levels have been adopted for ENSDF /29/.

However, only few levels of these are verified in their spectroscopical properties really. Ambiguous spin and parity assignments, unknown spectroscopical factors, deformation parameters and excitation strengths are oftenly met above 1 or 2 MeV excitation energy.

Any exact treatment of such a lot of discrete levels with doubtful spectroscopical characteristics is hopeless as well as from theoretical aspects and any practical application. Nevertheless, some attempts have been tried for the actual libraries ENDF/B-IV and JENDL-2 (see table 8). The relevance of such data is questionable because of they are based upon theoretical calculations purely. Four main reasons are responsible for the uncertainty in predicted excitation functions:

i) missing spectroscopical values E^*, I, π for the biggest part of all discrete levels;

Table 8: Discrete level structure for Lead accounted for by different libraries (excitation energy up to 4.36 MeV).

Library	Number of levels	Remarks on treatment
ENDF/B-IV	35 * **	including direct excitation contributions
JENDL-2	40 *	statistical model excitation functions only!
BROND (CJD)	35 *	smeared out by energy resolution function for representation as MF5 MT10 or as discrete levels in MF6 MT10
ENSDF	90	only quantum characteristics of levels

* Collapsing the total number of excited levels by grouping of neighbouring states

** Neglection of levels in the minor component ^{204}Pb

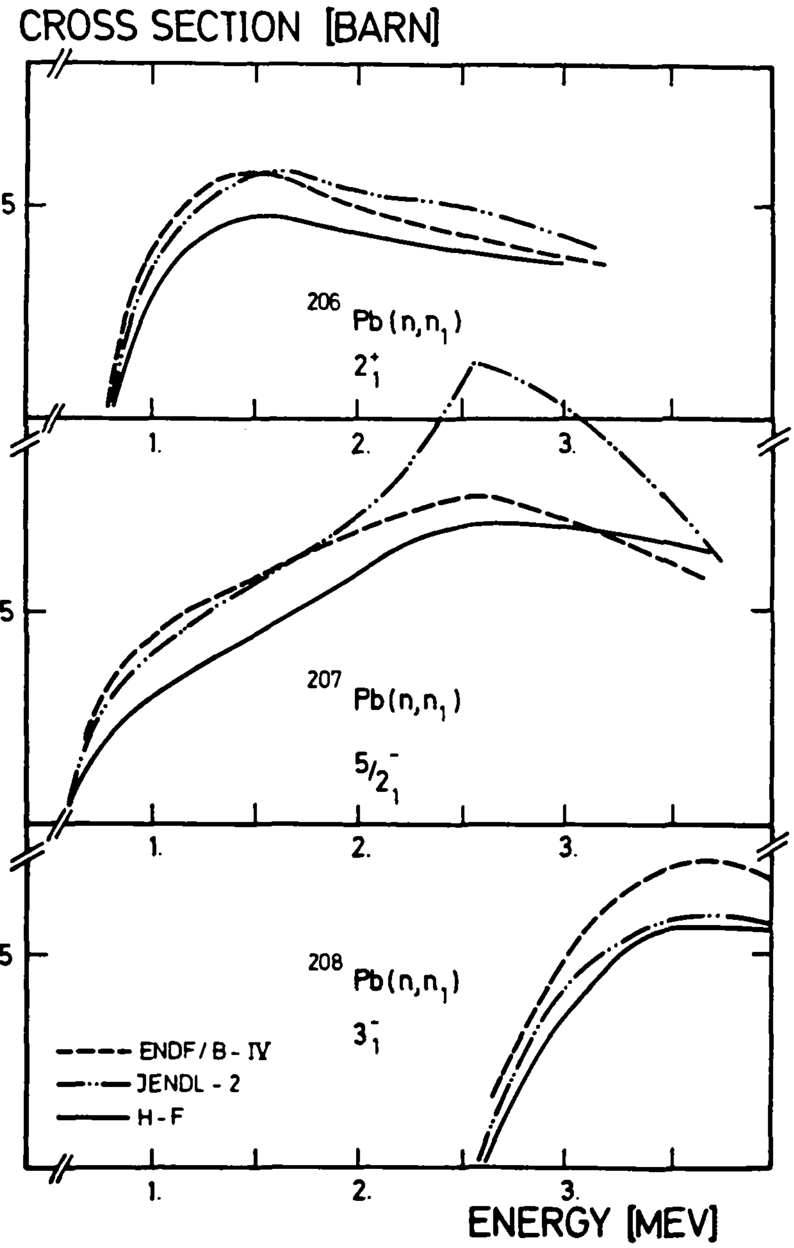

Fig. 10: Excitation functions for first excited levels in ^{206}Pb, ^{207,208}Pb near the threshold.

Calculations by Hauser-Feshbach formalism using Olssons potential /22/ are compared with evaluations for ENDF/B-IV and JENDL-2. Deviations in ^{207}Pb demonstrate the important effect of level-width-fluctuation corrections at energies near the threshold.

ii) level-width fluctuation corrections at energies just above the threshold up to 5 MeV in statistical model calculations (see fig. 10);
iii) contribution by direct excitation mechanisms at energies above 7 MeV calculated in the frame of collective models or coupled-channel-formalisms;
iv) absence of measured excitation functions for parameter adjustment for nearly all discrete levels other than the lowest few ones (see table 9).

For illustration in fig. 10 some excitation functions evaluated for different libraries are shown. Contributions from direct excitation mechanisms become relevant above 7 - 8 MeV. They have been accounted for by different approaches described in 2.3.1.2.

The evaluation of discrete level excitation for MAT 8201 has been performed as follows:

i) Adoption of evaluated data MT51 to MT87 from MF3 of ENDF/B-IV MAT1288 because also most recent optical potentials yield equivalent results (see fig. 10).
ii) Averaging of the δ-shaped functions by an effective energy resolution to construct a continuous spectrum for representation in MF5 MT10.
iii) Adoption of evaluated data from MF4 MT51 to MT87 of ENDF/B-IV MAT 1288 and representation in MF6 MT10.

2.3.1.2. Excitation of level continuum

Contributions from level continuum excitation to (n,n') will become the dominant process above 10 MeV incidence energy. About 80—90 % of neutron production goes via the excitation of overlapping levels in the intermediate nuclei including components of higher-order chance neutron emission from (n,2n), (n,pn), (n,αn), (n,3n) etc. additionally.

At 14 MeV the cummulative neutron spectrum is experimentally investigated very carefully /9,10,11,12/. Measurements of neutron spectra at energies 8 to 12 MeV are reported /30/ but data havn't been published anywhere up to now.

Table 9: Experimentally verified deformation parameters for the 3_1^- and 5_1^- levels in ^{208}Pb.

E/MeV	$\beta(3_1^-)$ Q = -2.615 MeV		$\beta(5_1^-)$ Q = -3.198 MeV	
7	0.137 ± 0.009	/5/	-	
11	0.130 ± 0.007	/7,8/	0.065 ± 0.005	/7,8/
20	0.123 ± 0.01	/5/	-	
22	0.124 ± 0.01	/5/	-	
24.5	0.108	/8/ *	-	
25.7	0.114 ± 0.007	/7,8/	0.064 ± 0.005	/7,8/
34	0.126	/8/ *	-	
40	0.11	/8/ *	-	
54	0.11	/8/ *	-	
61	0.103	/8/ *	-	

* derived from (p,p') experiments.

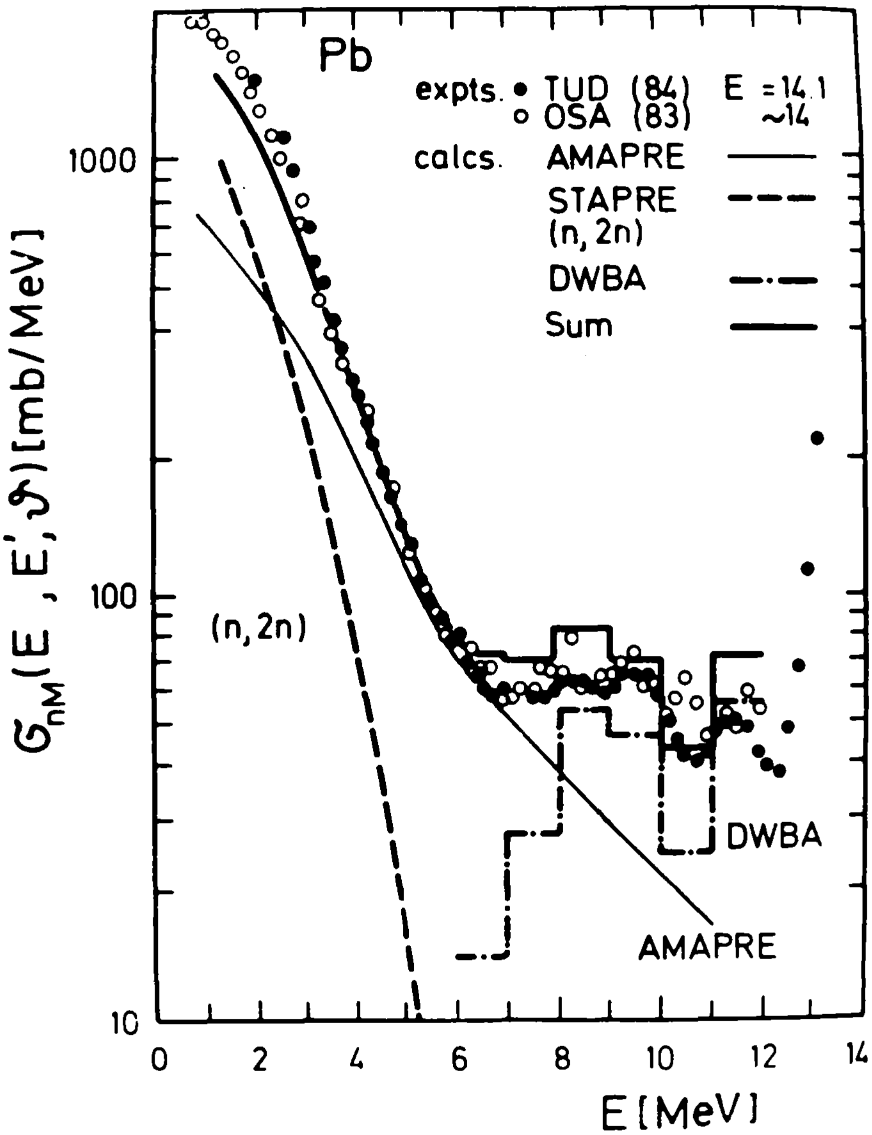

Fig. 11: Neutron production spectrum induced by 14 MeV neutrons. Experimental data /10,11/ are interpreted in terms of GEM (AMAPRE) and DWBA approaches of compound and direct reaction mechanisms.

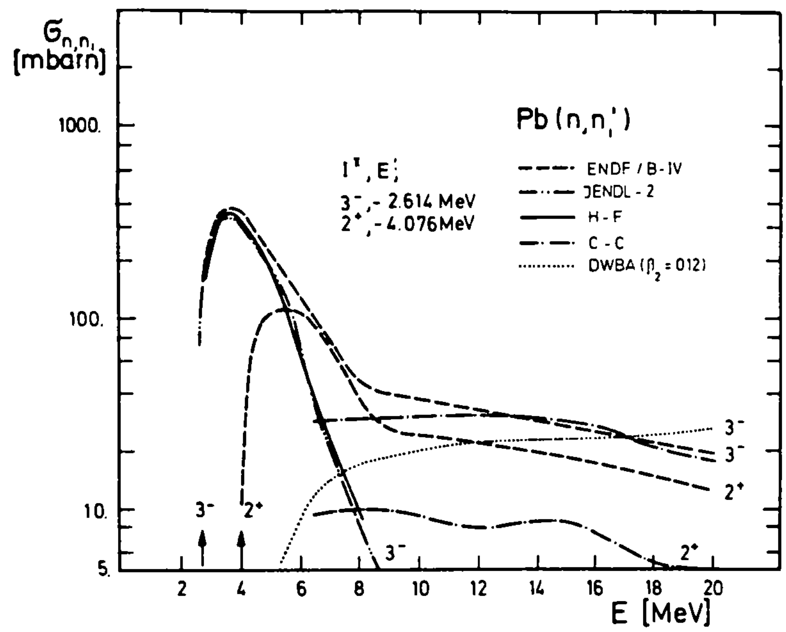

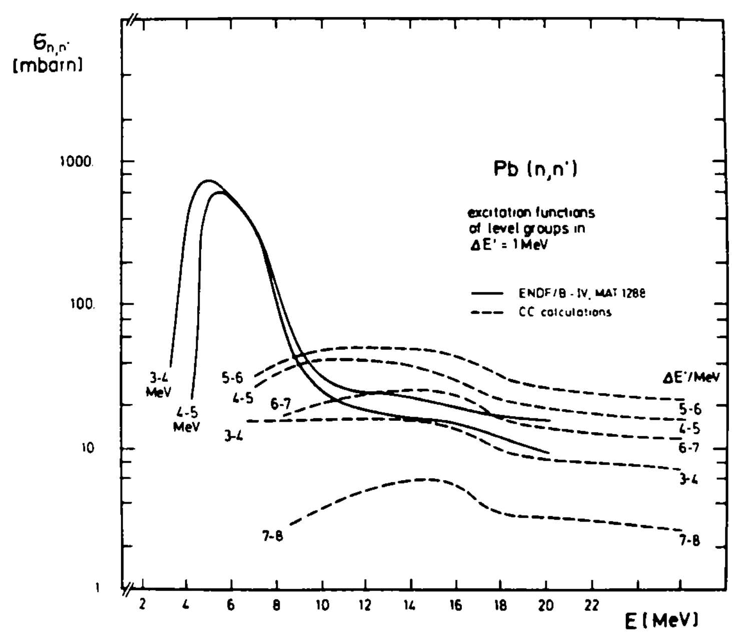

Fig. 12: Direct excitation contributions to neutron inelastic scattering to discrete levels (upper part) and level continuum (lower part).
Calculations for level continuum excitation have been performed in bin widths of 1 MeV of the excitation energy in a one-step phonon excitation approach for direct reactions in DWBA and CC-methods.

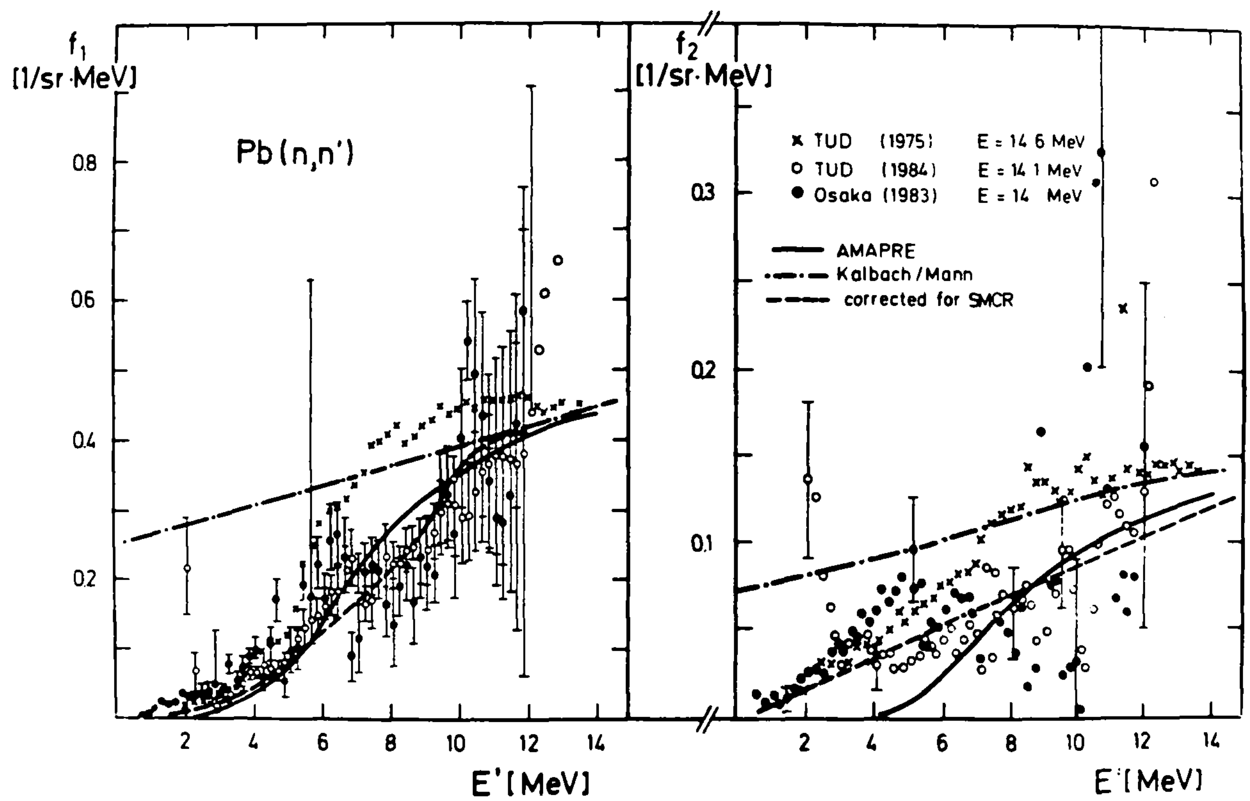

Fig. 13: First and second order Legendre polynomial coefficients for f_1 and f_2 the angular distributions of neutron emitted by 14 MeV neutron-induced non-elastic processes. Data extracted from experiments /9,10,11/ are well described by theoretical (AMAPRE) and semi-empirical (Kalbach-Mann) models. (Note different scales in ordinates for f_1 and f_2.)

Therefore, the evaluation of this important cross section is based on theoretical calculations checked by experimental data at 14 MeV. As visible in fig. 11 the neutron spectrum may be composed of at least two reaction mechanisms: compound nucleus processes and direct excitation modes. Calculations of spectra have been carried out in terms of the Generalized Exciton Model (GEM) which is a statistical appoach for Multi-Step-Compound (SMCR) and Multi-Step-Direct (SMDR) reactions simultaneously /17/. The computer code AMAPRE /17/ was used to perform these calculations.

Single-Step-Direct (1SDR) reaction contributions were approximated by DWBA taking into account collective excitations /16/. These calculations have been done for ^{208}Pb only in 1 MeV-bins of the excitation energy (see fig. 12). Important components of this excitation mode can be noted at high excitation energies.

By simple incoherent superposition of both components predicted by GEM and DWBA a surprisingly good agreement of experimental and theoretical data can be achieved at 14 MeV (compare fig. 11).

Analoguos calculations done for the incidence energy range from 5 to 20 MeV are based on this promising results at 14 MeV. All data have been represented by MT10 directly.

2.3.1.3. Angular distribution of primary emitted neutrons

In usual evaluated nuclear data files, angular distributions are given for discrete level excitation only whereas neutron emission via the level continuum in the intermediate nuclei is assumed to be isotropic generally in those files.

In MAT 8201 the anisotropy of neutrons emitted by non-elastic processes is provided for the first time. Basing on experimental data /9,10,11/ and theoretical calculations in the frame of the "Leading Particle Model" also implemented in the code AMAPRE, the angular distributions are parametrized by Legendre-polynomial coefficients $f_l(E,E')$ for $1 \leq l \leq 4$ /17,31/. The first and second order coefficients are shown in fig. 13 for 14 MeV neutron inelastic scattering.

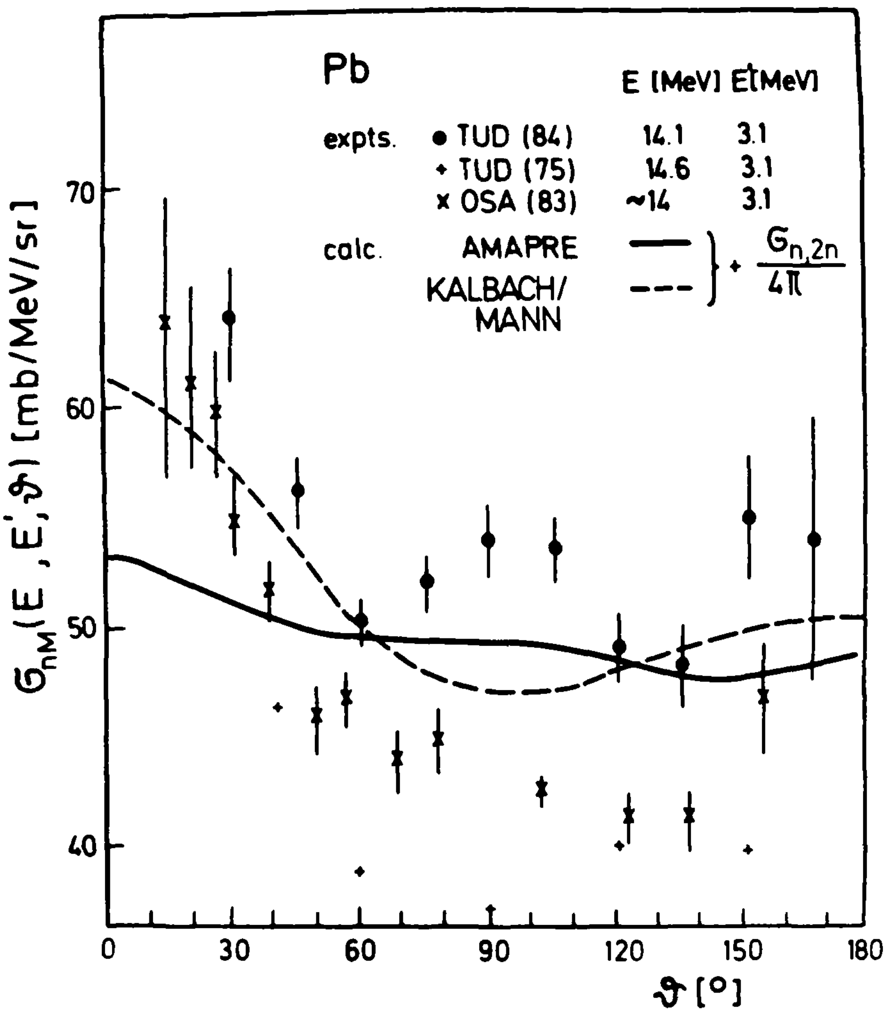

Fig. 14: Angular distribution of neutrons emitted with 3.1 MeV produced by 14 MeV neutron-induced non-elastic processes. Experimental data taken from /9,10,11/ can be described by GEM (AMAPRE) and the formalism of Kalbach/Mann.

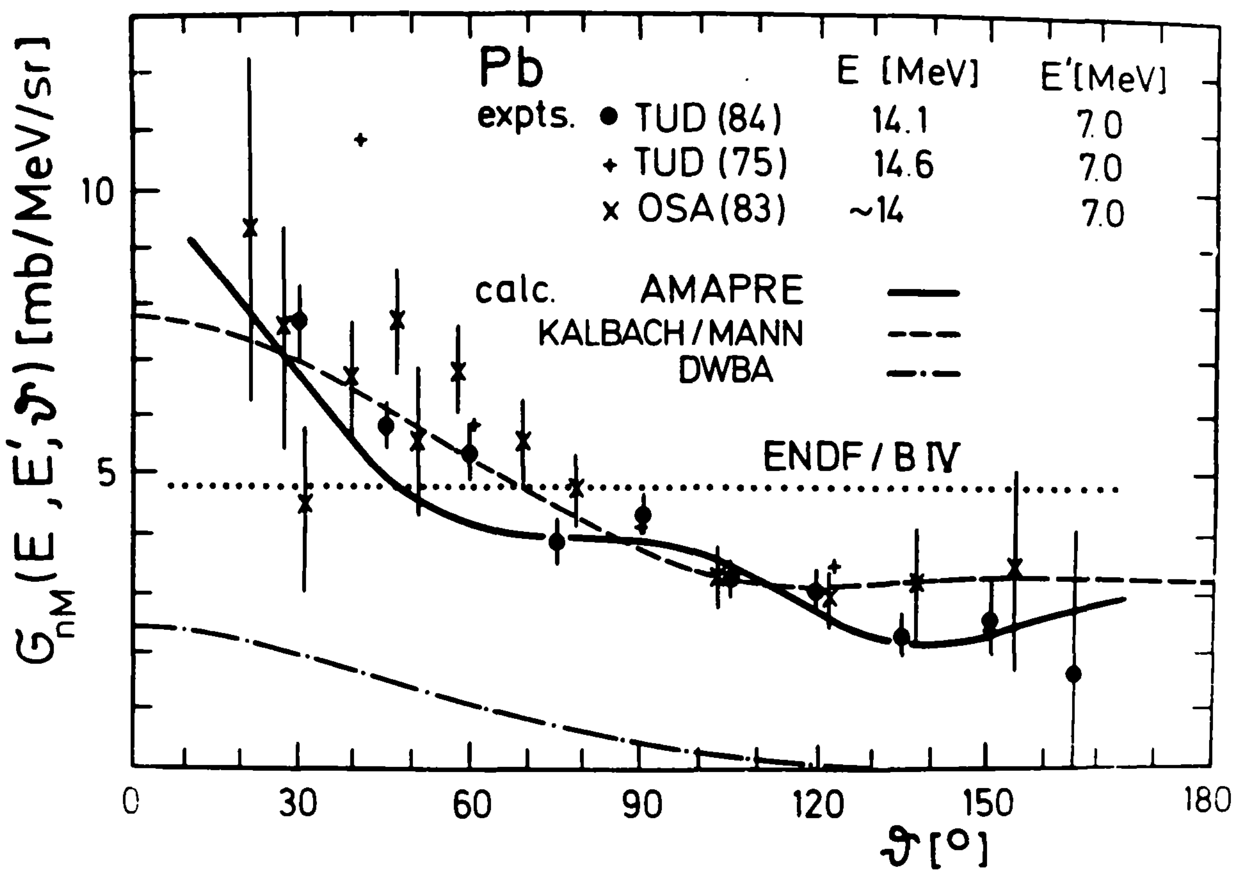

Fig. 15: Same as in fig. 14 for emission of 7-MeV neutrons. At this energy contributions from Direct reactions are small.

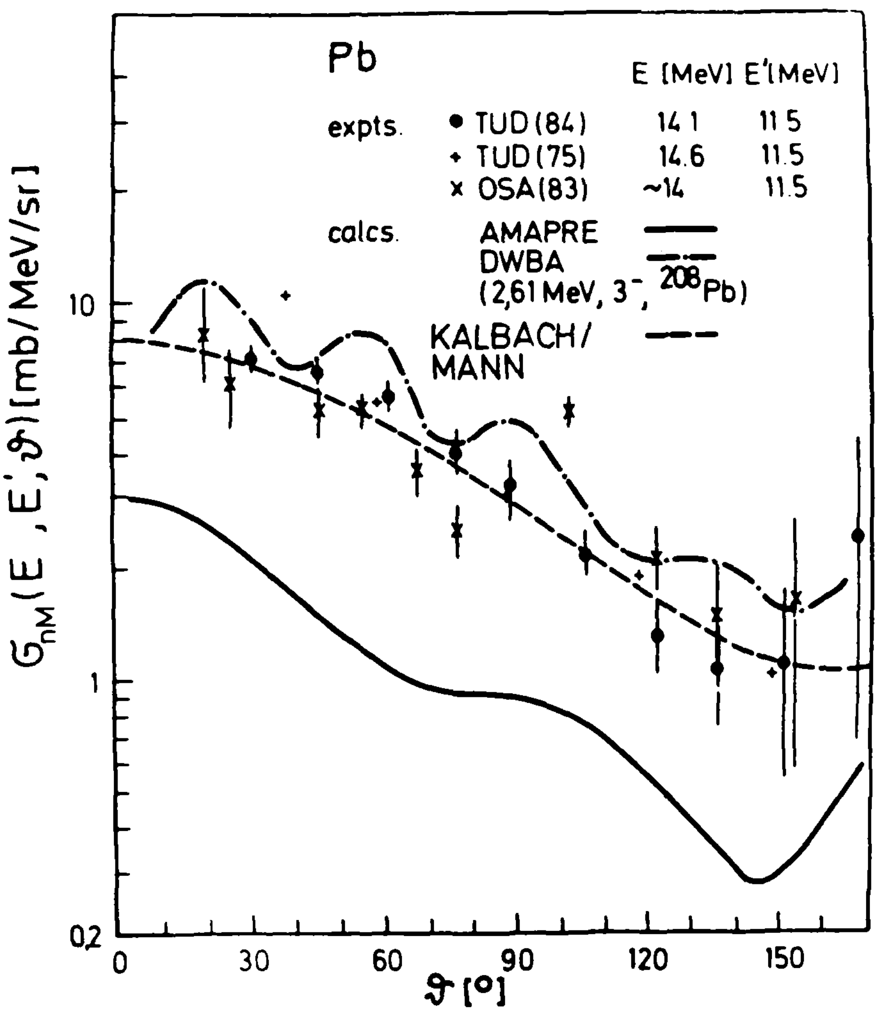

Fig. 16: Same as in fig. 14 for neutrons emitted with 11.5 MeV corresponding to the excitation of the (3_1^-)-level in ^{208}Pb.

According to this high emission energy the 1SDR component estimated by DWBA is the dominant reaction mechanism.

A surprisingly good agreement with angular differential experimental data can be achieved (see figs. 14,15,16) giving the argument for adoption of this method in the whole range from 5 to 20 MeV neutron incidence energy.

All data are represented in MF6 MT10 according to the recently recommended ENDF/B-VI rules and procedures /32/.

2.3.1.4. Total neutron inelastic scattering cross section

The determination of total inelastic scattering cross sections from experimental data requires necessarily:

i) integration over solid angle for angular distributions of discrete level excitation or double-differential cross sections;
ii) integration over excitation energy (or emission energy respectively); in the case of discrete level excitation this is equivalent to a sum over all levels excited.

Such numerical processing of experimental data results in increased uncertainties by following reasons in dependence on neutron incidence energy

$0 \leq E \leq 4$ MeV:

- limited angular range measurable in experiments;
- limited energy resolution hindering peak separation to derive all discrete level excitation cross sections.

$4 \leq E \leq 10$ MeV:

- continuum level excitation becomes dominant with increasing energy requireing measurements of neutron spectra with low detection thresholds ($E_{thr} \lesssim 100$ keV) to ensure small corrections resulting from extrapolation of E' to 0. on the basis of theoretical models.

$10 \leq E \leq 20$ MeV:

- contributions from (n,2n), (n,3n) and other neutron producing reactions can't be separated experimentally. Therefore (n,n') cross sections are based on theoretical models only.

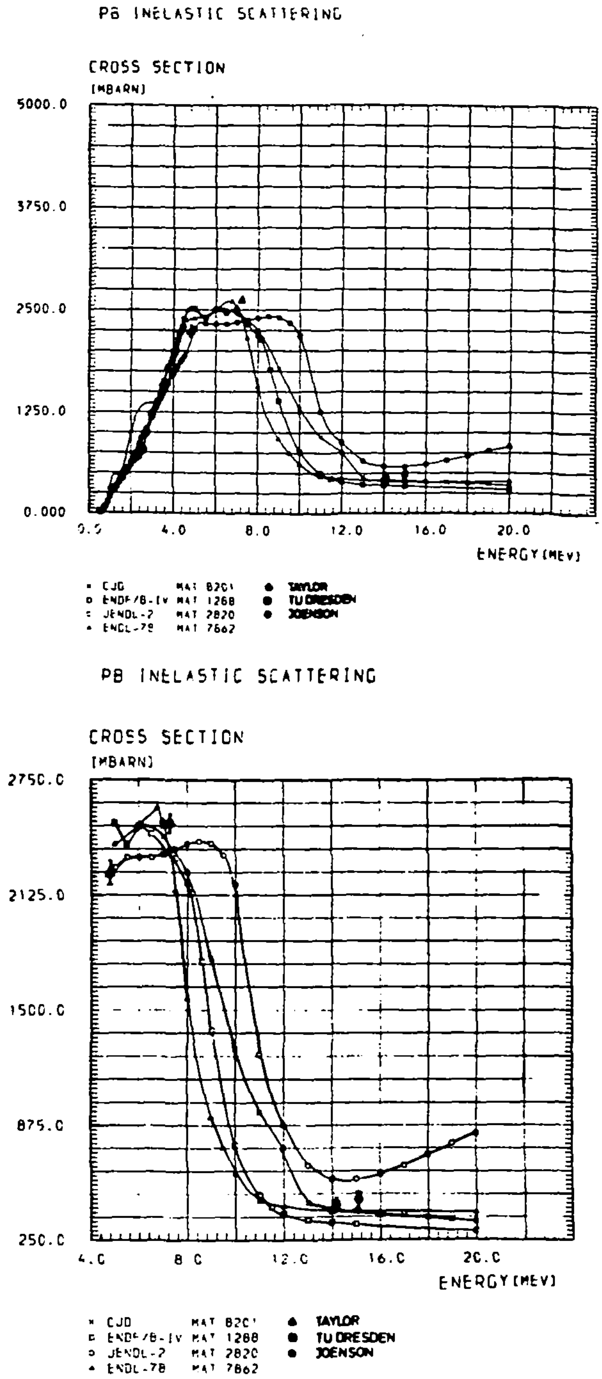

Fig. 17: Inelastic neutron scattering cross sections
upper part: low energy range including discrete level excitation.
lower part: high energy range determined by continuum level excitation (MT91) mainly.

These problems result from insufficient experimental data for (n,n') cross sections reflected by quite different evaluations available for this quantity (see fig. 17).

Also cross sections predicted by theoretical models are more or less reliable keeping in mind problems like:

i) the determination of optical model parameters and the level widths fluctuation correction factors at moderate energies ($E < 4$ MeV);
ii) the determination of direct mechanism contributions to statistical models usually applied;
iii) the determination of branching for one-particle and/or multi-particle-emission determined by the level-density parameters for the intermediate and residual nuclei respectively.

Results obtained from Hauser-Feshbach-Model calculations purely are demonstrating those aspects (compare fig. 17).

For file 8201 MT4 have been obtained by adopting ENDF/B-IV data matched at 5 MeV to calculations in terms of statistical models (STAPRE, AMAPRE).

2.3.2. (n,2n) cross sections and secondary neutron emission spectra

The (n,2n) reaction cross sections are of highest priority for application (neutron multiplication in hybrid reactor blanket arrangements).

The present knowledge of this quantity is assumed to be inadequate to fulfill nuclear data requests (compare table 10 and fig. 18).

Therefore, a critical analysis and re-evaluation is proposed for other libraries /4,33/ consequently.

Since earlier evaluations some new measurements has been carried out at 14 MeV /13,34,35/ and for the smaller energies /13/.

Unfortunatly, recently measured and published data can't remove existing ambiguities totally by the facts

i) Frehaut /13/ published values deviating by about 10 % without any comment (table 10);

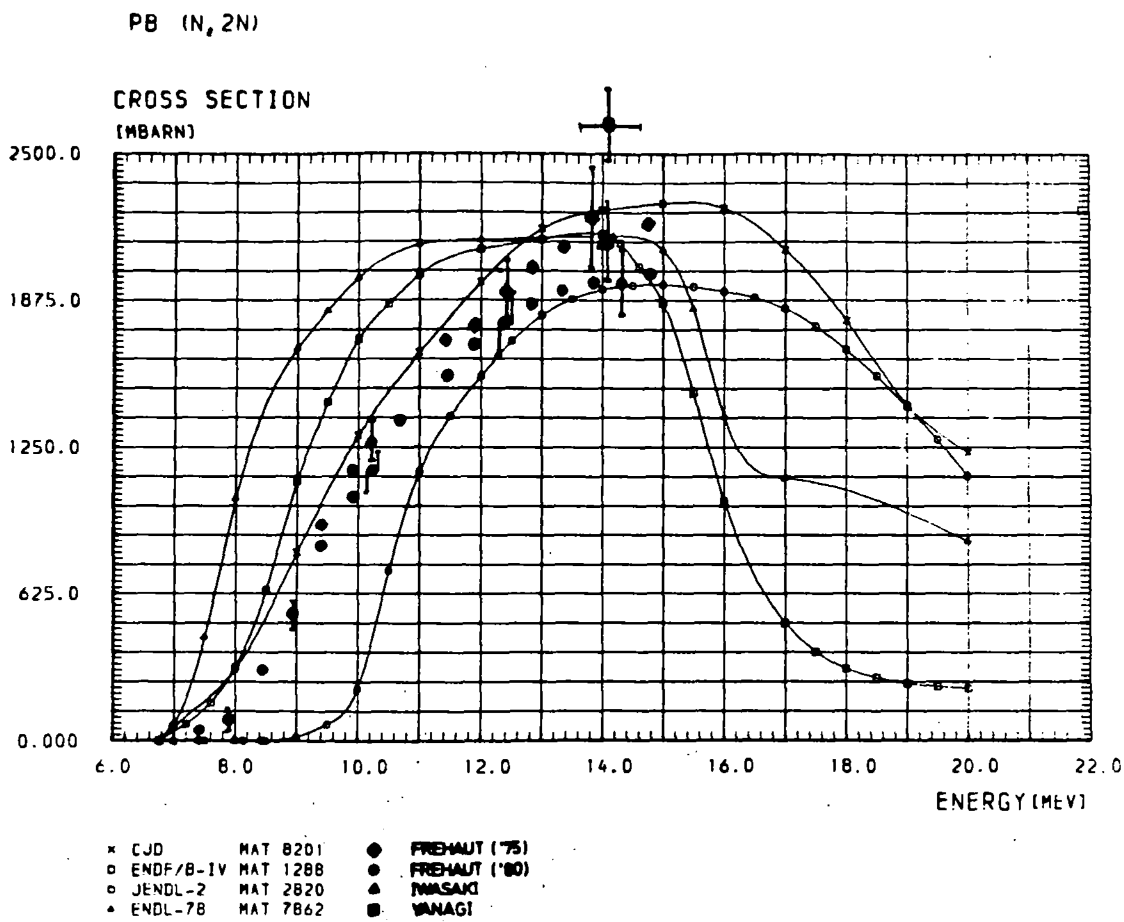

Fig. 18: (n,2n) reaction excitation function.
Recommended data for various libraries are compared with experimental results obtained by Frehaut et al. /13/.

Table 10: (n,2n) cross section (in barns) obtained by Frehaut et al. /13/.

E/MeV	published in ZfK-324	published in BNL-NCS-51245	difference (in %)
7.41±0.165	-	0.042±0.031	-
7.93±0.15	-	0.104±0.015	-
8.44±0.135	-	0.299±0.023	-
8.94±0.125	-	0.530±0.036	-
9.44±0.115	0.934±0.044	0.835±0.044	12
9.93±0.11	1.162±0.054	1.044±0.054	11
10.19±0.105	1.275±0.059	1.148±0.059	11
10.74±0.095	-	1.386±0.072	-
11.44±0.09	1.722±0.083	1.566±0.083	10
11.88±0.085	1.780±0.088	1.707±0.085	4
12.36±0.085	1.945±0.129	1.782±0.129	9
12.85±0.08	2.033±0.136	1.869±0.136	9
13.33±0.075	2.111±0.143	1.924±0.143	10
13.80±0.075	2.260±0.154	1.961±0.154	10
14.28±0.07	-	1.953±0.142	-
14.76±0.065	2.235±0.156	2.006±0.156	12

Table 11: (n,2n) cross sections (in barns) at 14 MeV determined experimentally by different authors.

Author Year	E/MeV	$\sigma_{n,2n}$	Method/ Remarks
Graves /36/ 1955	14	2.490±0.02	Flux measurement
Ashby /37/ 1958	14.1	2.650±0.2	n-coincidences
Lebedev /38/ 1958/59	14	2.460±0.1	Flux measurement relative to $^{63}Cu(n,2n)$
Flerov /39/ 1958/59	14	2.300±0.19	Flux measurement
Adam /40/ 1963	14	1.800±0.2	n-coincidences (may be 20-30 % lower due to correlations) → 2.0...2.15
Joensson /41/ 1969	15.1	2.000±0.3	competition of (n,3n) results in small value
Mather /42/ 1969	14.1	1.936	
Maslov /43/ 1972	14.2	2.24	
Frehaut /13/ 1975(30)	14.76 ±0.065	{2.235±0.156 2.006±0.156	see table 10
Iwasaki /34/ 1982	14.8	2.130±0.25	n-spectra at different angles integrated from 0 to 6 MeV
Yanagi /35/ 1984	14	2.640±0.16	n-spectrum from 80 keV to 6.4 MeV (13-17 % to high) → 2.20...2.30

ii) Yanagi's results can be assumed to be too high by 13 - 17 % in comparison to ENDF/B-IV /33,35/.

Examing this situation by independent calculations with the statistical model code STAPRE strong evidence are given for higher values given by Frehaut /13/ at earlier time (see fig. 18) adopted for MAT 8201. At 14 MeV an estimated value of 2.26±0.10 barns can be derived in agreement with corrected experimental results.

Independently an analysis was carried out by Carmona and Yiftah /44/ starting from experimental excitation functions for separated isotopes 204, 206, 207, ^{208}Pb. All data could be interpreted in terms of the semi-empirical Segev-Model /45/ by a slight adjustment of reaction thresholds. For the natural isotopic composition of Lead following cross sections can be deduced at 14 MeV:

$$\sigma_{n,2n} = 1.964 \text{ barns} \quad /44/$$
$$\sigma_{nX} = 2.25 \text{ barns} \quad /44/ \quad .$$

The latter cross section is too small by about 200 to 300 mbarns (compare fig. 28) and may also be understood as an indication for a systematical shift in Frehauts' data of 10 to 15 % (compare table 10) additionally. Finally, the systematics of (n,2n) cross sections at 14.1 MeV calculated by Pearlstein /46/ gives

$$\sigma_{n,2n} = 2.47 \text{ barns} \; .$$

A critical review of the influence of pre-compound neutron emission on the (n,2n) cross section Holub et al. /47/ confirm the decrease of theoretical cross sections by the factor

$$\frac{\sigma^{exp}_{n,2n}}{\sigma^{Pearlstein}_{n,2n}} = (-3.79 \pm 2.45) \cdot 10^{-4}\, A + (0.947 \pm 0.037)$$

at an excitation energy of the residual nucleus of $U_R \approx 6$ MeV. For the important isotopes of Lead (206, 207, 208) this condition is fulfilled yielding a factor of 0.87±0.09.

Table 12: Recommended (n,2n) cross section (in barns) at 14 MeV

Author/ Library	$\sigma_{n,2n}$ obtained	corrected and recommended
Yanagi /35/	2.64 ± 0.16	2.33 ± 0.13
Pearlstein /46/	2.47	2.15 ± 0.22
Carmona /44/	1.964	2.20 ± 0.05
this work MAT 8201	2.26 ± 0.10	2.26 ± 0.10
ENDF/B-IV		2.167
ENDL-78		2.150
ENDL-82		
UKNDL-80		2.260
JENDL-2		1.921
BROND (CJD)		2.260

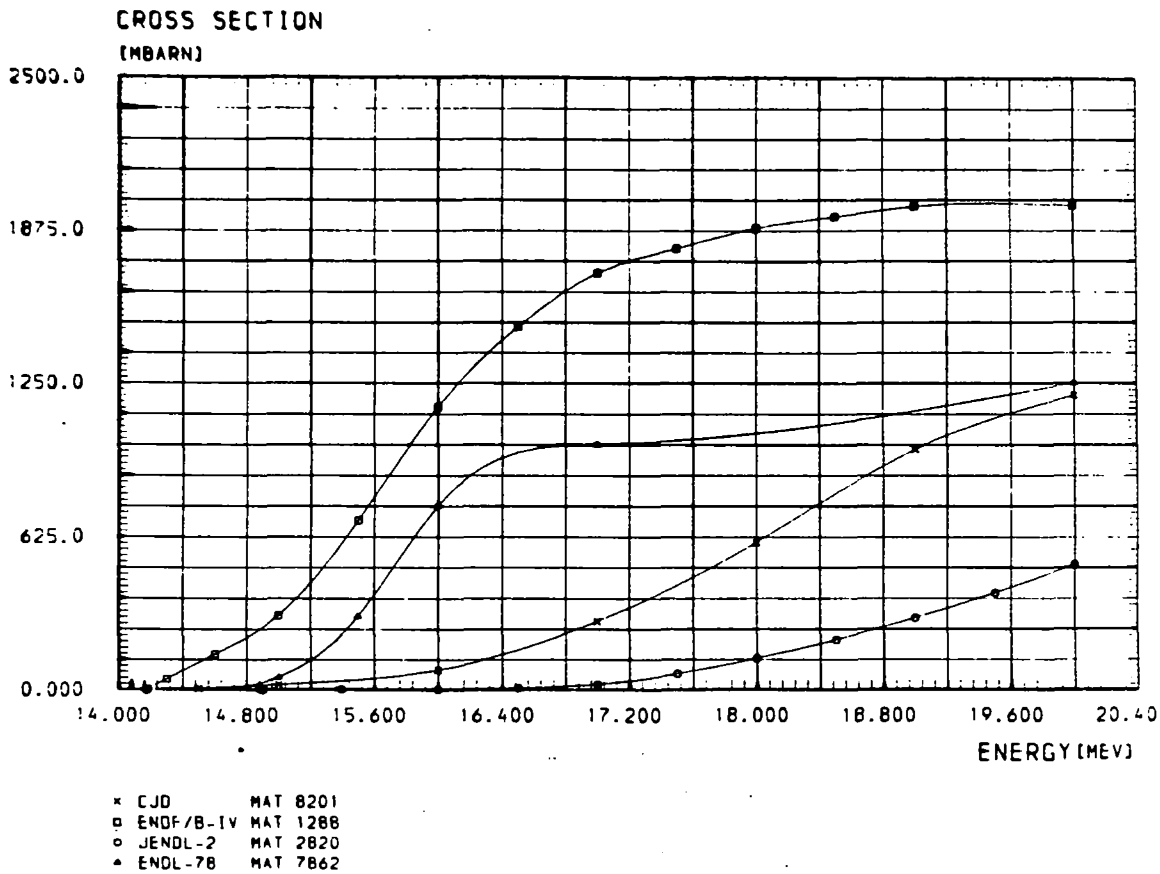

Fig. 19: (n,3n) reaction excitation function.
Recommended data are compared.

In table 12 all results obtained from critical analysis of the (n,2n) cross section at 14 MeV have been compiled together with those values adopted in evaluated data libraries.

Energy spectra of secondary emitted neutrons have been calculated by the code STAPRE. Experimental data at about 14 MeV have been used to check these theoretical results of course, angular distributions of secondary neutron emission has been assumed to be isotropic in good agreement with experiments /35/.

2.3.3. (n,3n) reaction cross sections

Up to now, no data for (n,3n) excitation function are available. Therefore all evaluations are based upon theoretical calculations only resulting in strongly deviating recommendations (see fig. 19). Data for MAT 8201 have been derived from calculations with code STAPRE which yields considerably smaller values than in MAT 1288 of ENDF/B.

2.3.4. Further neutron emitting reaction cross sections

Above the (n,np), (n,pn), (n,nα) and (n,αn) reaction thresholds only small contributions to the neutron emission spectra can be expected. Nevertheless, they should be estimated by theoretical calculations using the code STAPRE too.

Reaction cross sections for these channels are included under MT10 in MF3 and MF5 respectively.

Data for (n,pn) and (n,αn) have been given under MT719 and 799 separatly.

In figs. 20 and 21 the excitation functions recommended by different authors (or libraries) are shown.

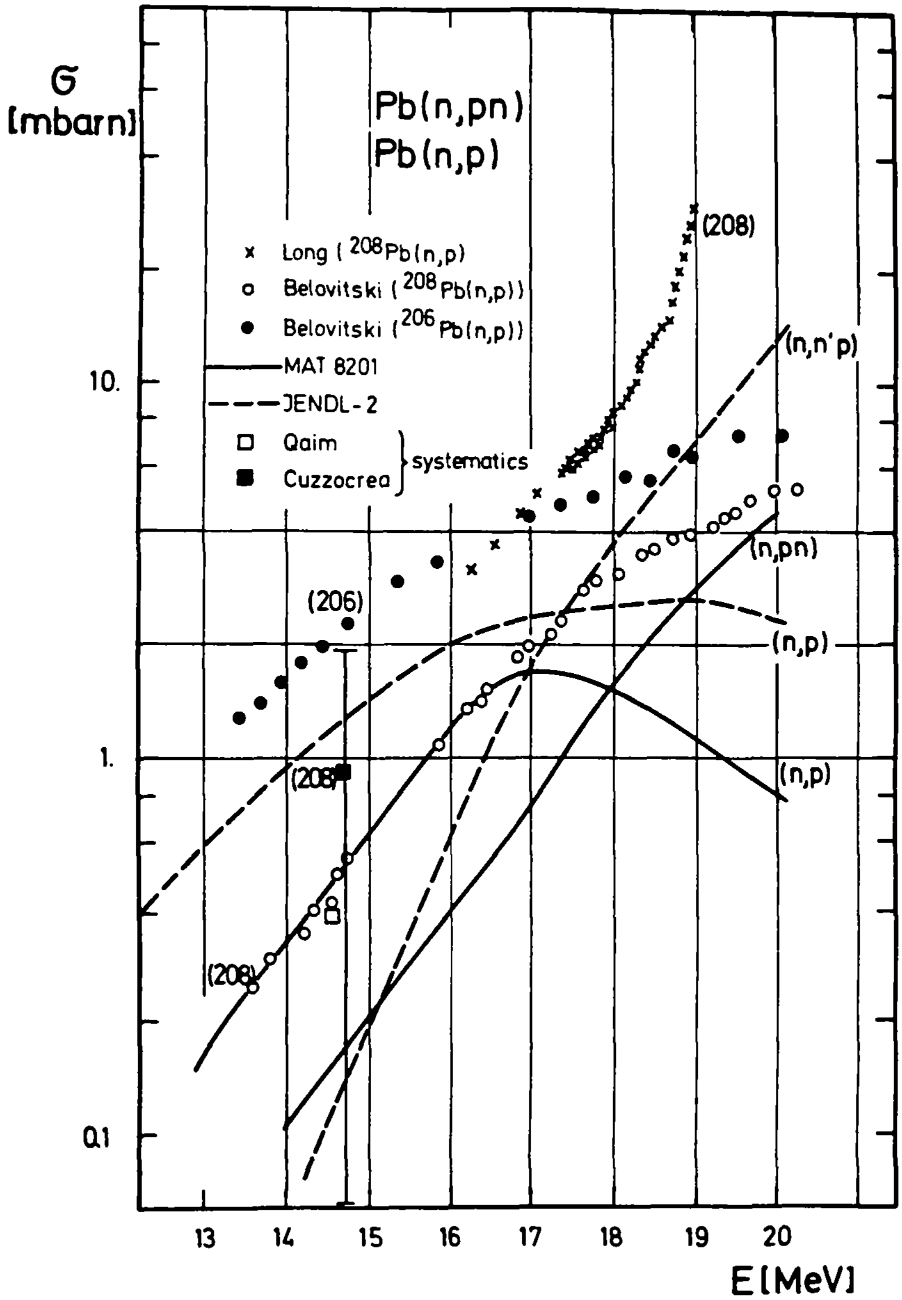

Fig. 20: Proton production cross section.
Evaluations are compared with experimental results.
Data points derived from experiments and systematics have been taken from refs. /52/ and /53,54/ respectively.

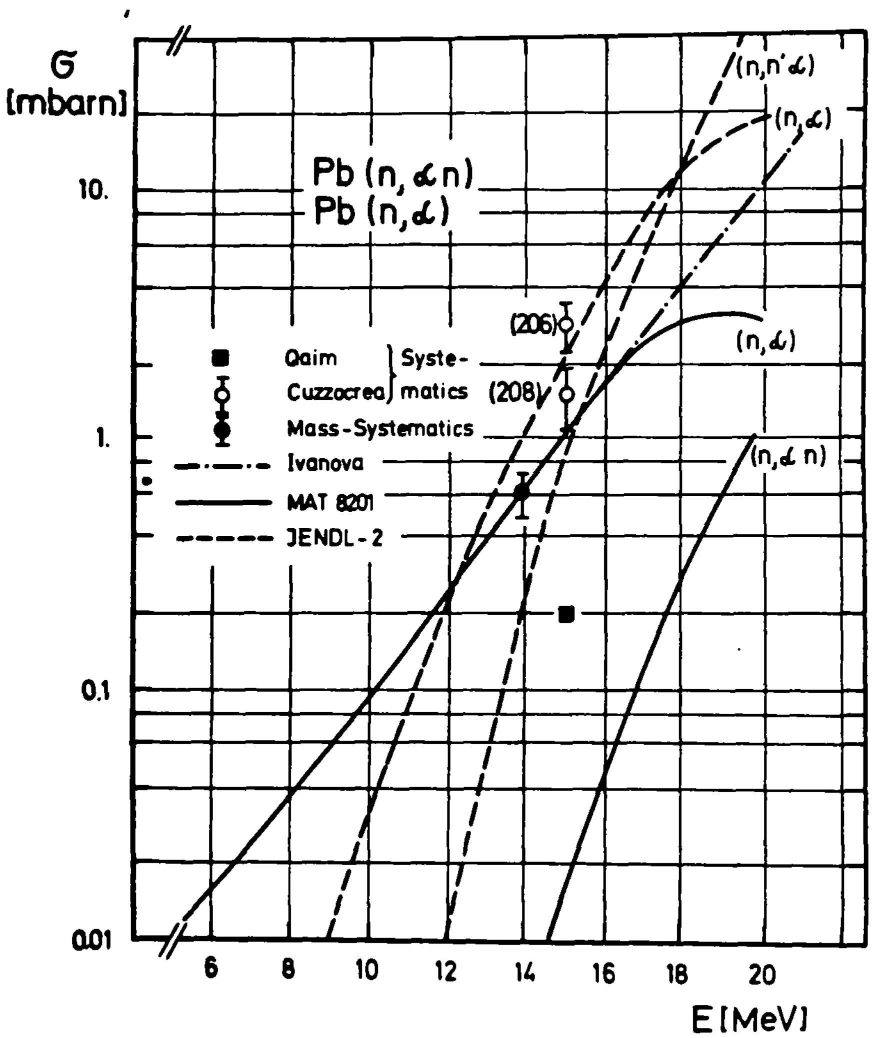

Fig. 21: Alpha-particle production cross section.
Evaluations are compared with experimental results and systematics taken from refs. /53,54/ and /56/ respectively.

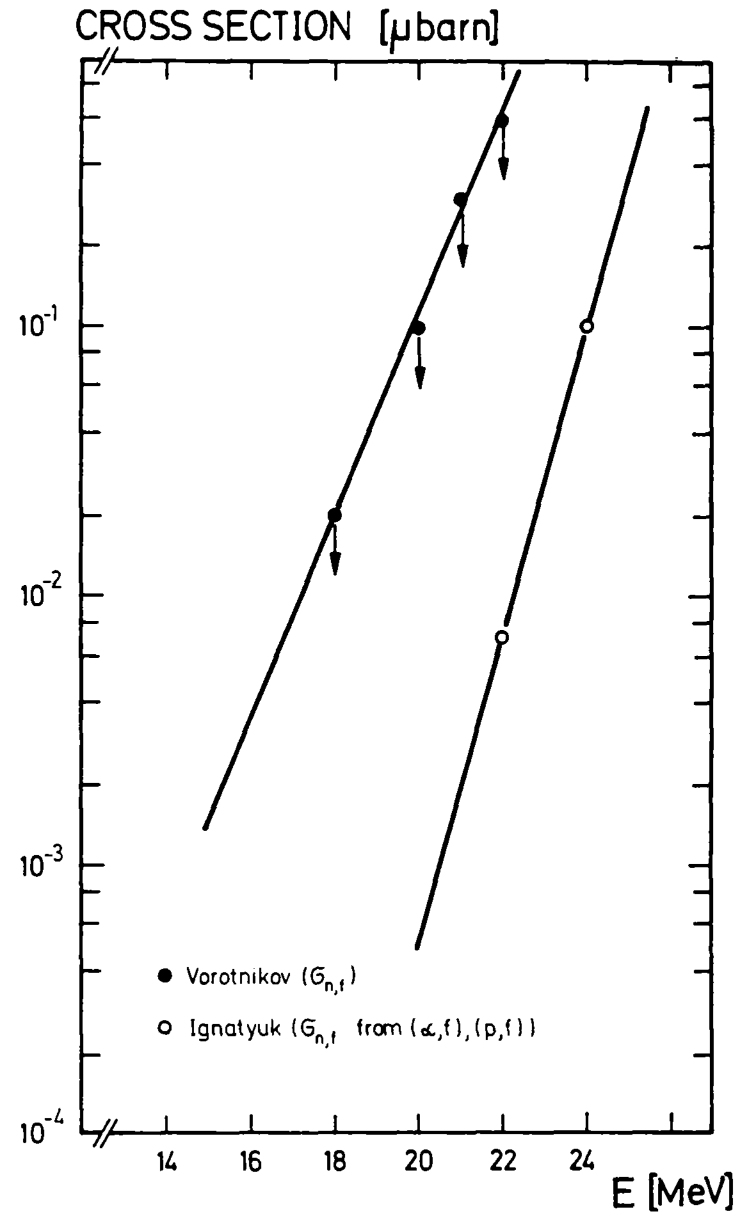

Fig. 22: Neutron-induced fission cross section.
Experimental data have been taken from refs. /48,49/.

2.3.5. Neutron-induced fission cross sections

Recently the neutron-induced fission of ^{nat}Pb has been investigated experimentally /48/ but only upper cross section limits could be derived for the energy range from 18 to 22 MeV (see fig. 22).

On the other hand from independent (α,f) and (p,f) experiments realistic cross sections have been determined by Ignatyuk and Shuravlev /49/. Therefore, a crude estimation yields a value of about 0.001 μbarn at 20 MeV.

Such small cross sections have no influence on the neutron production cross section balance really. They have been ignored in MAT 8201 totally.

2.4. Neutron absorption reactions

2.4.1. Neutron capture cross sections

Neutron capture cross sections have been evaluated according to three energy ranges:

i) thermal energy range from 10^{-5} eV to 1 keV;
ii) resolved resonances region from 1 keV to 1.6 MeV;
iii) fast neutron energy region from 1.6 MeV to 20 MeV.

Generally, experimental data of neutron capture for isotopic or natural Lead are very scarce /50,51/. Therefore, different evaluations came to nearly identical conclusions.

The thermal region is characterized by a simple 1/v-dependence valid up to an energy of about 10 to 100 eV at least fitted by a constant c according to

$$\sigma_{n,\gamma} = c / \sqrt{E}$$

(E in eV, c in barns). The values obtained for c are tabulated in table 13.

Table 13: 1/v-dependence for neutron capture in Lead according to the relation $\sigma_{n,\gamma} = c / \sqrt{E}$ (E in eV).

Isotope	c/barns
^{204}Pb	0.14±0.04
^{206}Pb	0.0475
^{207}Pb	0.11±0.01
^{208}Pb	0.00007
^{nat}Pb	0.0282±0.002

Table 14: 2200 m/s - cross section for neutron capture in Lead.

Library/ Reference	$\sigma_{n,\gamma}$/barns
ENDF/B-IV	0.198
JENDL-2	0.1716
BROND (CJD)	
/52/	0.170±0.02

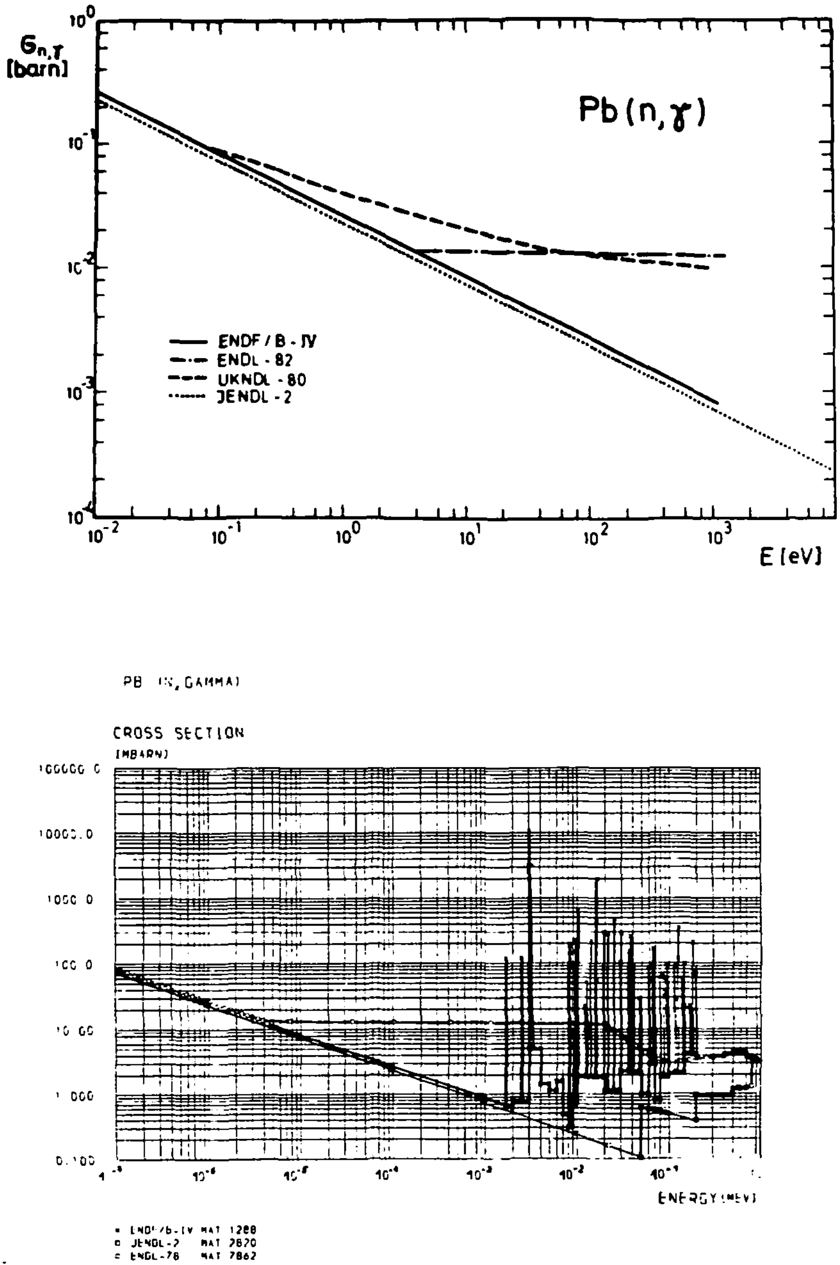

Fig. 23: Capture cross sections in the low energy region.

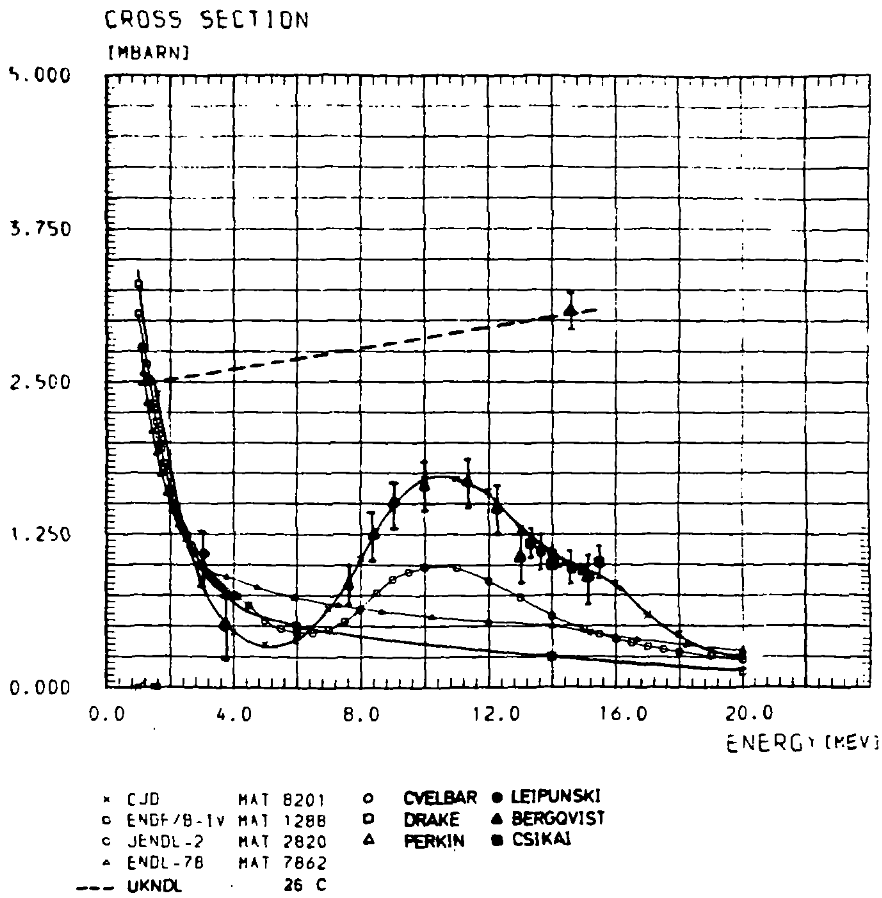

Fig. 24: Fast neutron capture cross sections.
Experimental data have been taken from BNL-325 /51/.

A 2200 m/s-value results from this in the order of 0.17 to 0.20 barns (see table 14).

The resonance region is highly structured by more than 100 resolved resonances. However, unfortunatly for only 15 % of all resonances radiation widths could be determined experimentally. Therefore, averaged values of known radiation widths have been used.

All results and the comparison with other libraries are shown in fig. 23.

Fast neutron capture is a process having small cross sections. Nevertheless an exact knowledge of both the cross section and the corresponding γ-quanta spectrum is of practical importance in neutron transport calculations for radiation shielding because of the presence of very high γ-ray energies up to 20 MeV and more.

In fig. 24 all experimental data available at present are summarized and compared to previous evaluations and recent calculations carried out by use of codes FISPRO and PEQGM for MAT 8201.

2.4.2. Charged-particle production cross sections

2.4.2.1. Proton emission cross sections

Proton emission cross sections have been measured recently for separated Lead-isotopes by Belovitskij et al. /52/. These data confirm an experimental value $\sigma_{n,p} = 0.96 \pm 1$ mbarn obtained by activation technique at 14.8 MeV /53/.

The extrapolation within a $\sigma_{n,p}$-mass-systematics which is defined in a range of the asymetry parameter $0. \leq (N-Z)/A \leq 0.15$ yields a value of 0.4 mbarn /54/ in fair agreement with Belovitskij's results.

Therefore, calculations with code STAPRE have been adjusted to interprete these data to form recommended values given in MAT 8201.

In fig. 20 both experimental and evaluated data for (n,p) are shown for fast neutron energies above 10 MeV.

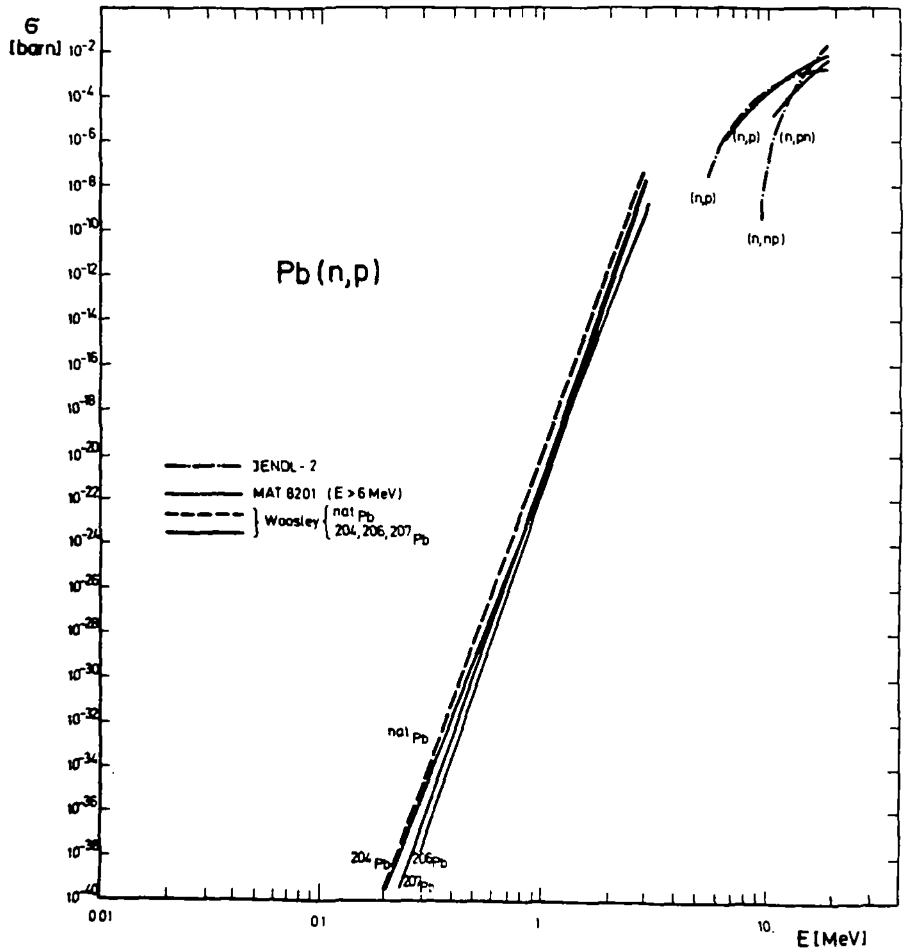

Fig. 25: (n,p) reaction excitation function.
Theoretical calculations in the frame of H-F-formalism have been performed by Woosley et al. /55/ near the threshold and for MAT 8201 in the high-energy region.

Below 10 MeV strongly decreasing but non-vanishing cross sections can be expected because of positive Q-valued (n,p) reactions for Lead isotopes. Calculations carried out by Holmes et al. /55/ have been adopted for MAT 8201 in the low-energy region. All results have been represented in fig. 25.

Proton spectra and angular distributions havn't been included in MAT 8201.

2.4.2.2. Alpha-particle emission cross sections

The experimental knowledge on (n,α) cross sections are even worser than for the (n,p) reaction. Cuzzocrea /53/ compiled two values obtained by activation measurements at 14.8 MeV for ^{206}Pb ($\sigma_{n,\alpha}$ = 2.7±0.4 mbarn) and ^{208}Pb ($\sigma_{n,\alpha}$ = 1.58±0.25 mbarn).

Basing on a mass-systematics derived by Qaim /54/ from experimental data in a range $0.0 \leq (N-Z)/A \leq 0.15$ an estimate for Lead ($(N-Z)/A \approx 0.21$) can be extrapolated in a firster order only giving 0.2 mbarn at 14.7 MeV. This is much smaller than the value cited by Ivanova /56/.

However, there is no reliable matching point for an adjustment of statistical model calculations. Therefore, MAT 8201 adoptes results obtained by the theoretical study performed by Ivanova /56/. Alpha-particle spectra and energy spectra are not included in MAT 8201.

In figs. 21 and 26 the data are shown for the fast and slow neutron energies respectively.

2.4.2.3. Deuteron-emission cross sections

Basing upon the mass-systematics of cross sections for (n,d), (n,np) and (n,pn) reactions leading to the same residual nucleus a value of about 0.5 mbarns can be estimated /57/ at 14 MeV. Comparing this with data measured by proton spectrometry /52/ a vanishing cross section for (n,d) processes can be deduced at least within the experimental accuracy achieved.

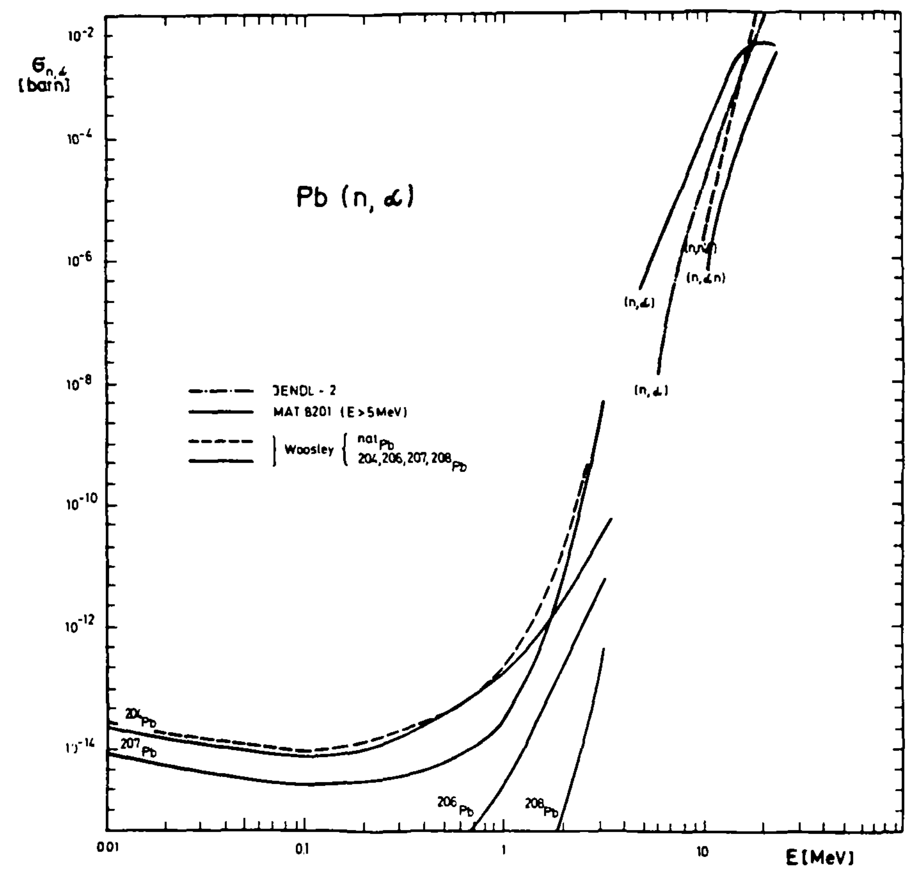

Fig. 26: (n,α) reaction excitation function .
Theoretically based calculations in terms of H-F-formalism have been performed by Woosley et al. /55/ and for MAT 8201.

Therefore, no data are given in MAT 8201.

2.4.2.4. Triton-emission cross sections

From the mass-systematics of $\sigma_{n,t}$ versus the asymmetry parameter (N-Z)/A at 14 MeV a value in the order of 20 μbarn /58/ can be estimated. Recently a value 30 ± 6 μbarn has been reported for ^{204}Pb /59/.

Such cross sections are of two orders of magnitude smaller than corresponding data for other charged particle production reactions and have been neglected in MAT 8201 consequently.

2.5. Non-elastic cross sections

Commonly, the evaluation of non-elastic cross sections proves a stringent consistency check for both

i) the sum of all partial reaction cross sections measured and calculated by various reaction mechanisms independently

and

ii) the difference $\sigma_{nT} - \sigma_{n,n}$ using experimental data and theoretical values derived from Optical Model calculations.

As usual too, more are less strong discrepancies appear between directly measured non-elastic cross sections and those deduced from experimental data for σ_{nT} and $\sigma_{n,n}$.

For natural Lead experimental values for the elastic scattering are very scarce /6,24,25,63/ and inconsistent at least in the energy range from 6 to 20 MeV (see fig. 27, upper part). At 14 MeV only one measurement is known /62/ yielding 2.83 ± 0.14 barns whereas a large body of experimental data for σ_{nX} exist resulting in an averaged value 2.50 ± 0.05 barn. The sum of both 5.33 ± 0.2 contrasts remarkable to the value of 5.5 ± 0.07 /63/ indicating a lack of cross section in the order of about 150 mbarns. Some arguments for an increased non-elastic cross section can be drawn from measurements by Taylor et al. /60/ and Degyarev et al. /61/ which permit a value of $\sigma_{nX} \sim$ 2.6 to 2.65 at 14 MeV. Such an increased non-elastic cross section

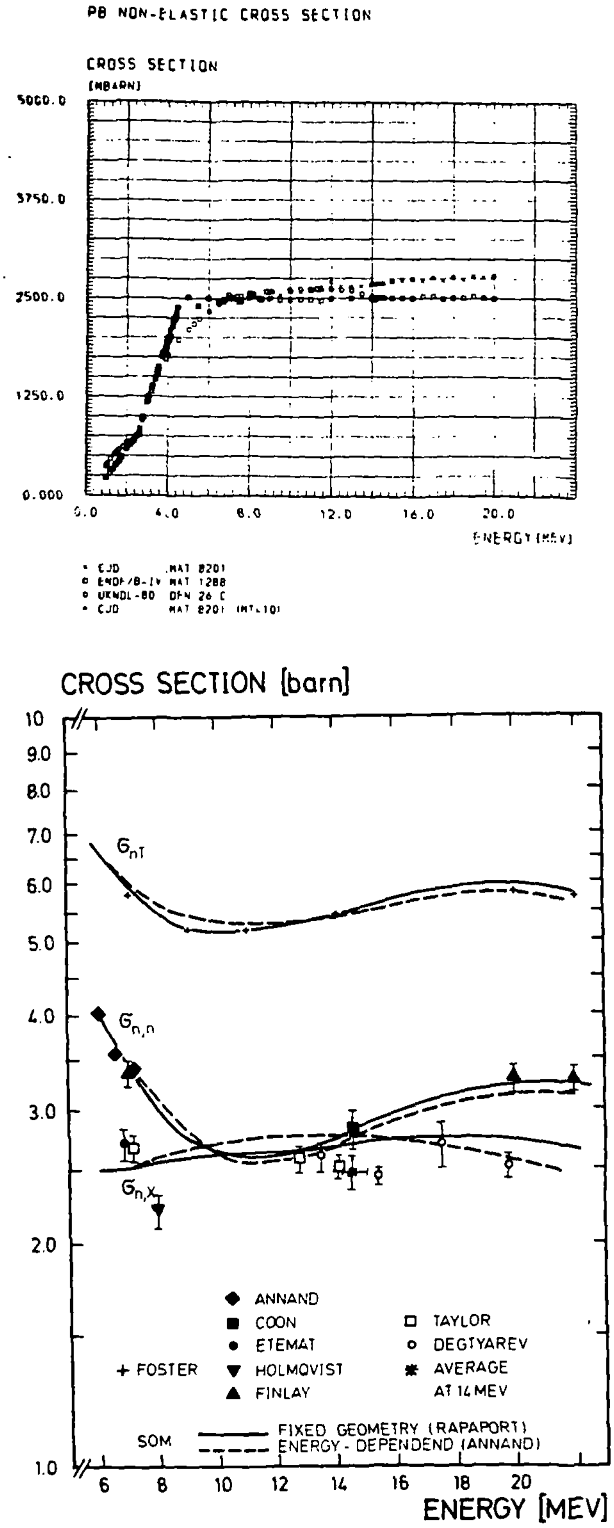

Fig. 27: Non-elastic cross section.
Upper part: Comparison of recommended cross sections given in various libraries.
Lower part: Consistency of experimental and theoretical data for σ_{nT}, $\sigma_{n,n}$ and σ_{nX}.

is in favourable agreement with a recent analysis of experimental elastic scattering data at 7, 20, 22 and 24 MeV done by Finlay et al. /6/ to determine Optical Model parameters. These parameters coincide with Rapaports' parameters /5/ adopted for the present evaluation fairly well. The results of Optical Model calculations basing on this potential have been included in fig. 27 too to demonstrate the consistency of experimental and theoretical results.

Very recently an anomaly in Optical Model parameter at neutron energies from 7 to 24 MeV has been pointed out by Finlay et al. /64/. Consequences of the energy dependence of geometrical parameters r_V, r_I and a_V found have to be investigated in the future.

Of course, the uncertainties in determination of non-elastic cross sections are clearly visible in the data included in various libraries too (compare fig. 27, lower part).

Any final acceptance of evaluated non-elastic cross sections is guided by the consistency with the corresponding difference $\sigma_{nT} - \sigma_{n,n}$ which can be estimated independently.

This problem has been already discussed and demonstrated in figs.2 and 3.

So, the uncertainties of this data type can be derived directly.

2.6. Parameters for resolved resonances

The resonant part of structured cross sections (σ_{nT}, $\sigma_{n,n}$, $\sigma_{n,\gamma}$) can be parameterized in terms of Multi-Level-Breit-Wigner resonances (MLBW). A compact storage of such parameters has been provided for by the ENDF/B-format rules.

Generally, such parameters (E_r, s_r, π_r, Γ_r, $\Gamma_{\gamma r}$, Γ_{nr}) are known partially. In most cases the total width Γ_r have been derived from experiments only /65,66/ resulting in uncertainties in the corresponding neutron and γ-widths (Γ_{nr} and $\Gamma_{\gamma r}$ respectively). Such a set of resonances parameters have to be carefully checked to reproduce the related quantity $g\Gamma_{nr}\,\Gamma_{\gamma r}\,/\,\Gamma_r$ correctly. This quantity represents the contribution from capture cross sections to the resonance integral.

Table 15: Statistics of MLBW-parameters in MAT 8201.

Isotope	Abundance (in %)	Energy range (in keV)	Number of resonances			
			l=0	l=1	l=2	total
^{204}Pb	1.4	1.33 - 103.	44	54	-	98
^{206}Pb	24.1	3.3 - 896.	35	140	190	365
^{207}Pb	22.1	3.0 - 472.	12	94	16	122
^{208}Pb	52.4	70. - 1735.	2	15	7	24
^{nat}Pb	100.0	10^{-8} - 1600.	93	303	213	609

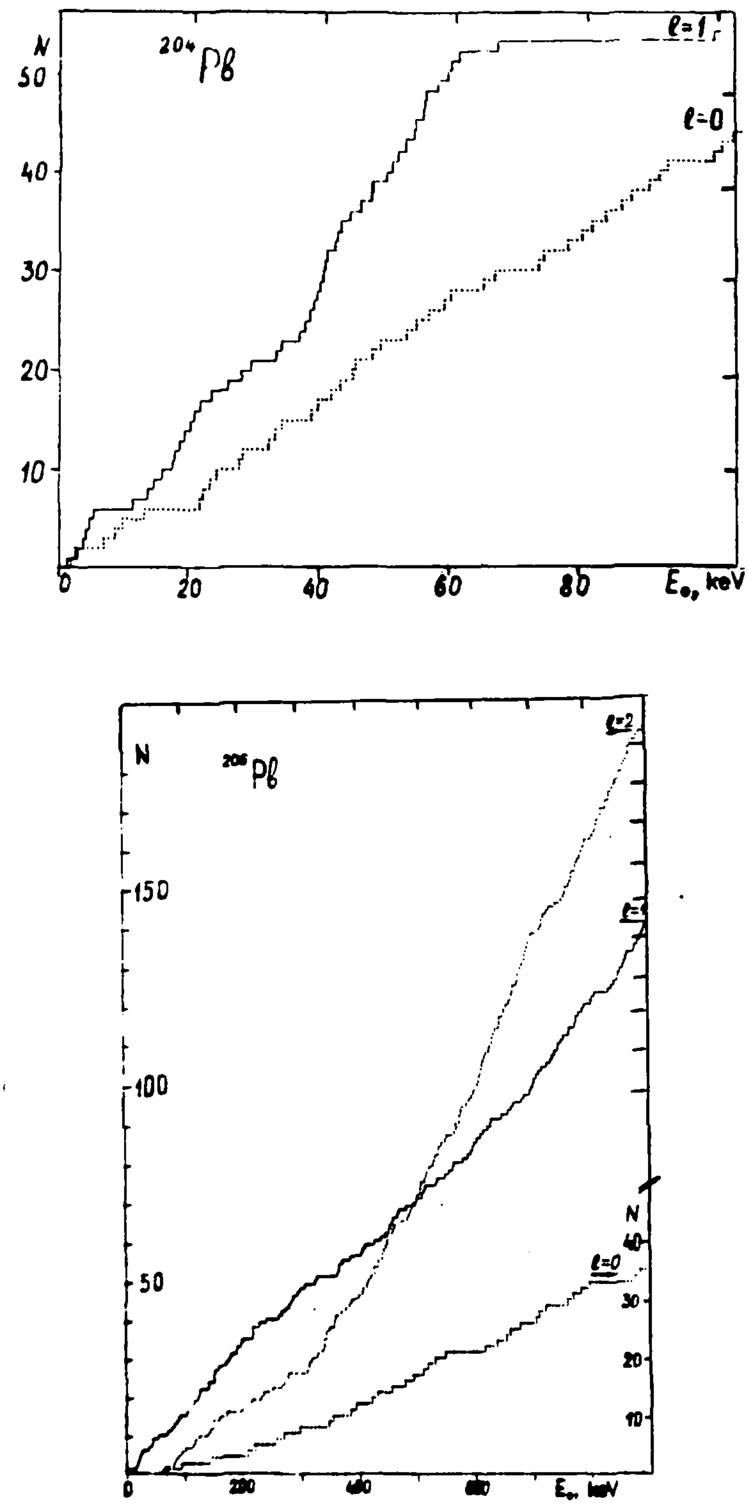

Fig. 28: Cummulative sum of resolved resonances in the composite nuclei ^{204}, ^{206}Pb+n.

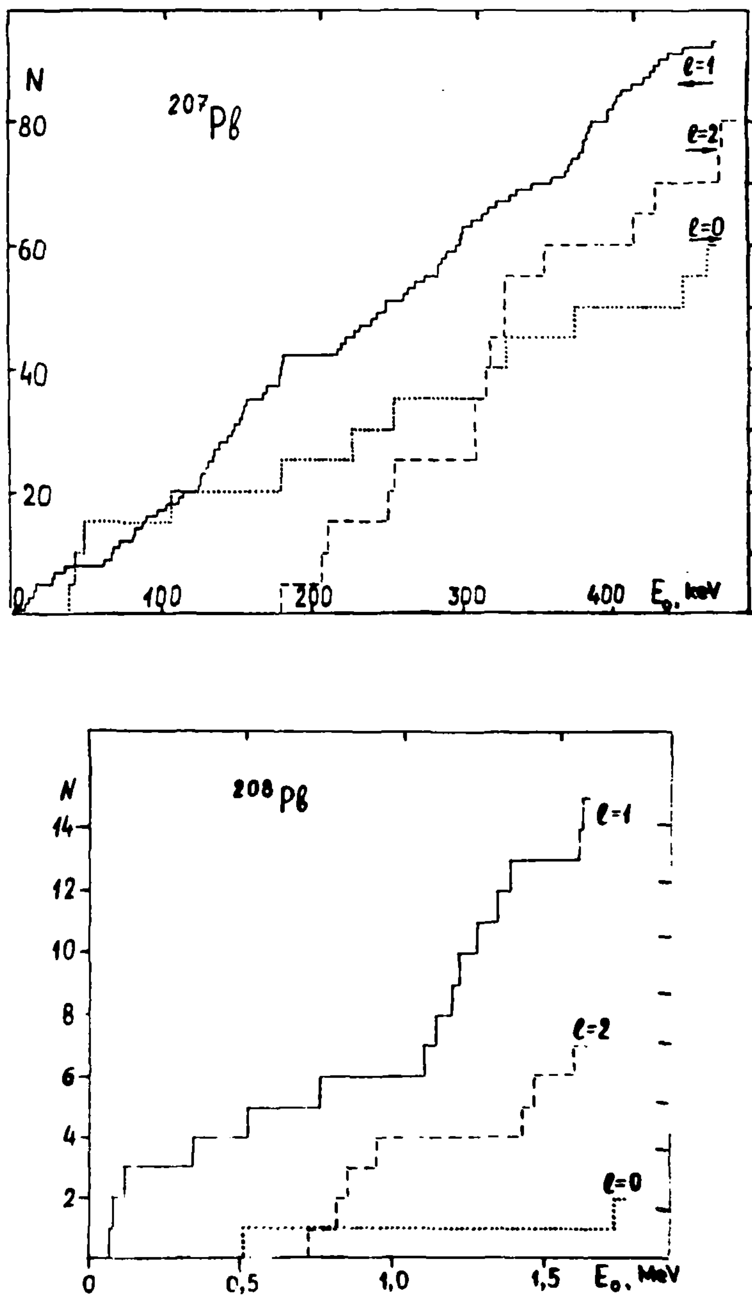

Fig. 29: Same as in fig. 28 for $^{207,\ 208}$Pb+n.

In table 15 the number of resolved resonances adopted for $^{204, 206, 207, 208}Pb$ have been summarized. All parameters results from analysis of neutron cross sections compiled in /65/ or carried out by Horen et al. /66/ recently. For resonances with unknown radiation widths averaged values $\overline{\Gamma_\gamma}$ have been assumed for each isotope and angular momentum individually.

Resolved resonances parameters have been given in different energy ranges choosen for Lead isotopes individually too.

The corresponding upper energy limit of these ranges were defined by that energy where a remarkable loss of experimentally determined resonances (especially p-resonances) is observed. This is obviously visible in the cummulative sums of resonances shown in figs. 28 and 29 giving energies of about 60 keV for ^{204}Pb and roughly 600 keV for $^{206, 207}Pb$.

Beyond these energies the cross sections for all three isotopes are given using unresolved-resonances-parameters extracted from these cummulative sumes too which yields averaged distances $\bar{D}$ between neutron resonances directly.

The energy dependence of averaged widths of resonances $\overline{\Gamma}$ necessary to represent unresolved resonances have been estimated by use of the statistical model implemented in the code EVPAR /67/. From this code also the radiative strength functions can be obtained additionally. These quantities may be directly compared with those extracted from analysis of averaged radiation widths and cummulative sums of experimentally observed neutron widths of resolved resonances. The latter quantities are shown in figs. 30 and 31 for all isotopes of Lead.

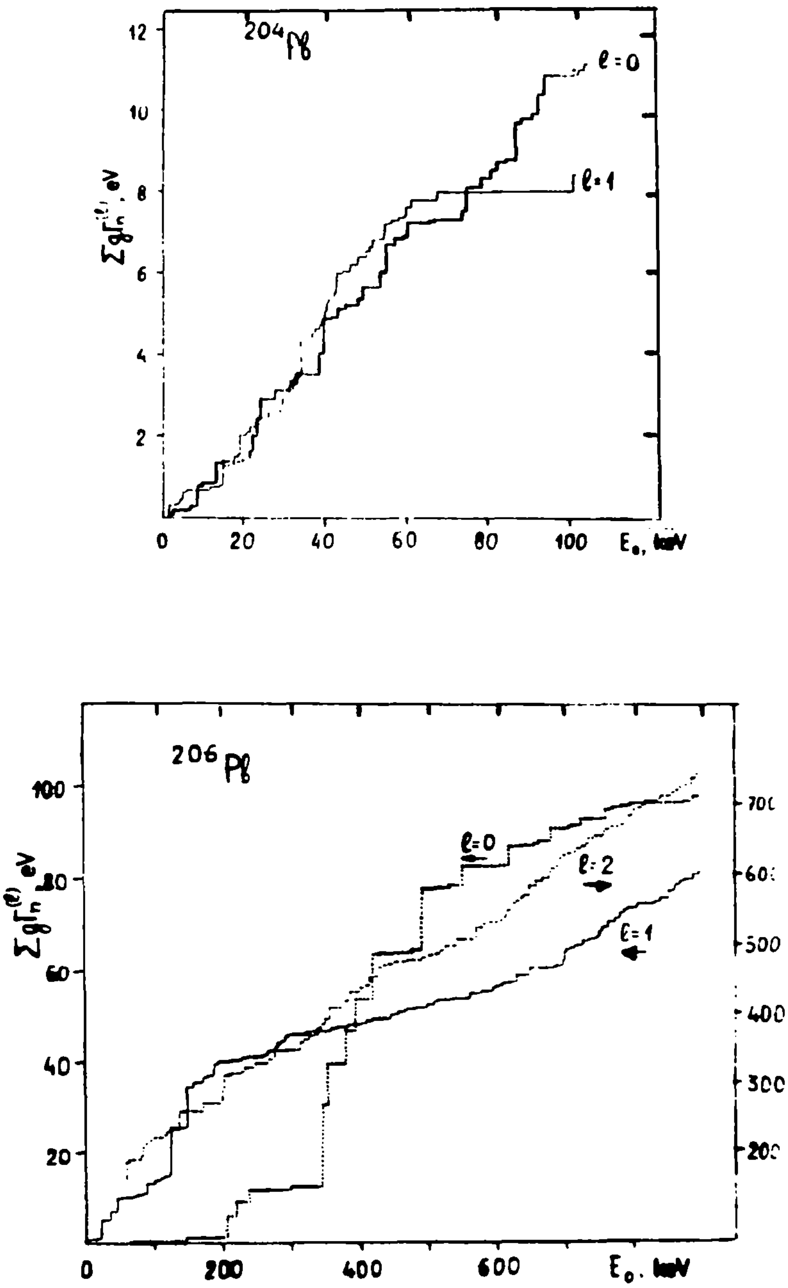

Fig. 30: Weighted cummulative sum of neutron widths for $^{204,\,206}Pb+n$.

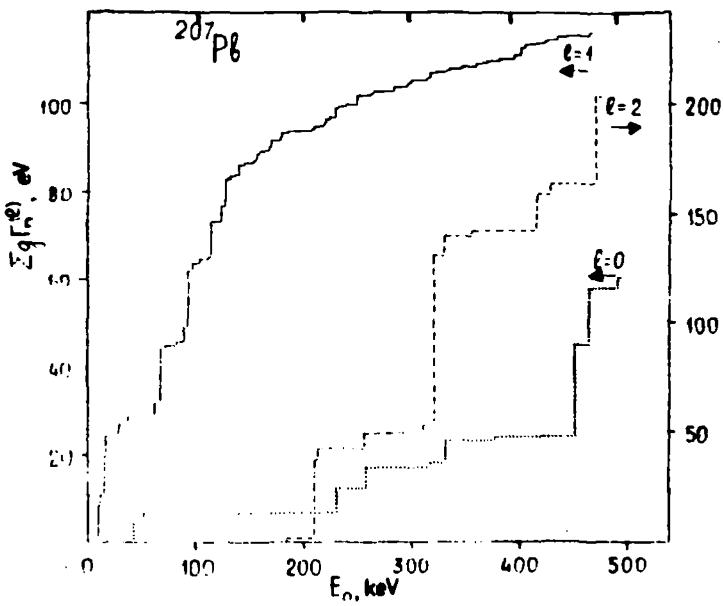

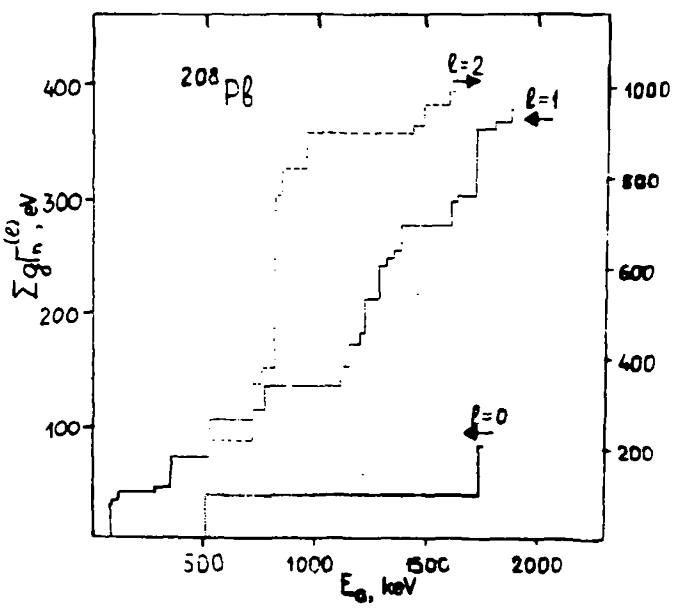

Fig. 31: Same as in fig. 30 for $^{207,\,208}$Pb+n.

3. Neutron-induced γ-ray emission cross sections

3.1. γ-ray production cross sections

For combined neutron- and γ-ray transport calculations it is desirable to include data for induced γ-ray emission in MAT 8201 too.

In an first attempt the adoption of cross sections evaluated for ENDL-78 (still valid for ENDL-82 and ENDL-84) was concluded.

The cross sections are stored in MF13 MT3 representing the total γ-ray production by non-elastic processes (see fig. 32).

3.2. γ-ray angular distributions

Considering angular distributions of γ-quanta clearly between discrete γ-lines and the continuous γ-background has to be distinguished.

The anisotropy of angular distributions for discrete γ-lines (γ-transitions between isolated states in the residual nucleus) has been well established for Lead isotopes too (for instance see ref. /68/ and original papers cited therein). The ratio of cross sections at 152^o and 90^o $\sigma(152^o)/\sigma(90^o)$ has been found to vary from 0.8 to 1.3 for $E_\gamma \sim 4$ to 5 MeV at neutron incidence energies from 5 to 7 MeV /68/.

On the other hand, continuously distributed γ-ray emission can be assumed to be emitted isotropically really.

By the reason that in MF13 excitation functions for discrete γ-ray emission are not given MF14 only reflects this isotropy of continuous γ-ray spectra.

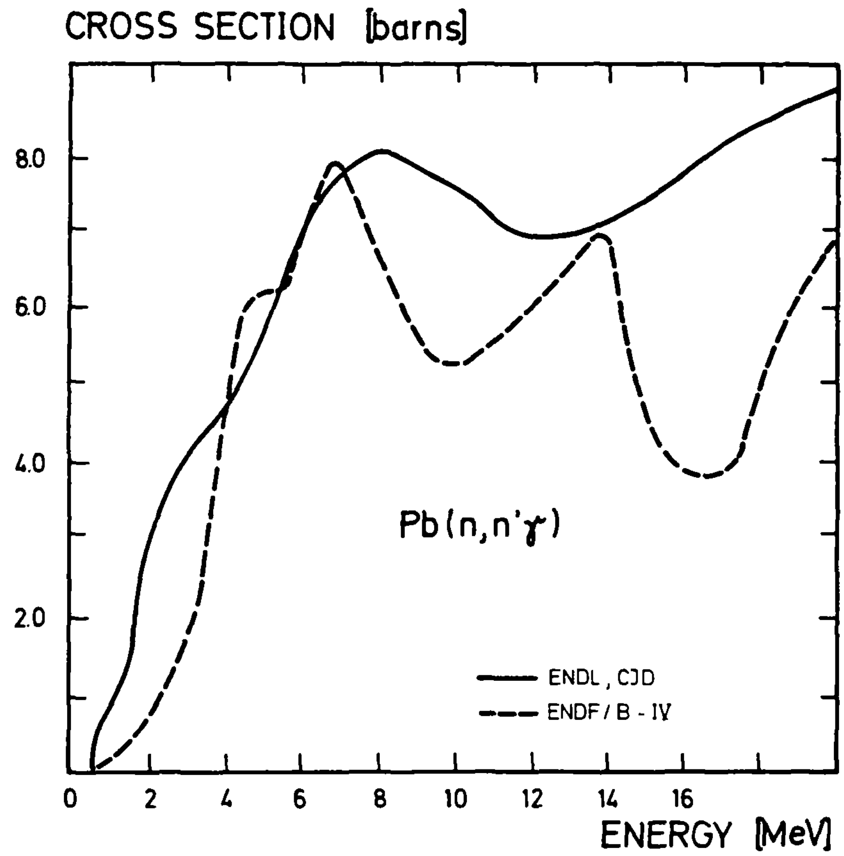

Fig. 32: γ-ray production cross section by neutron non-elastic processes.

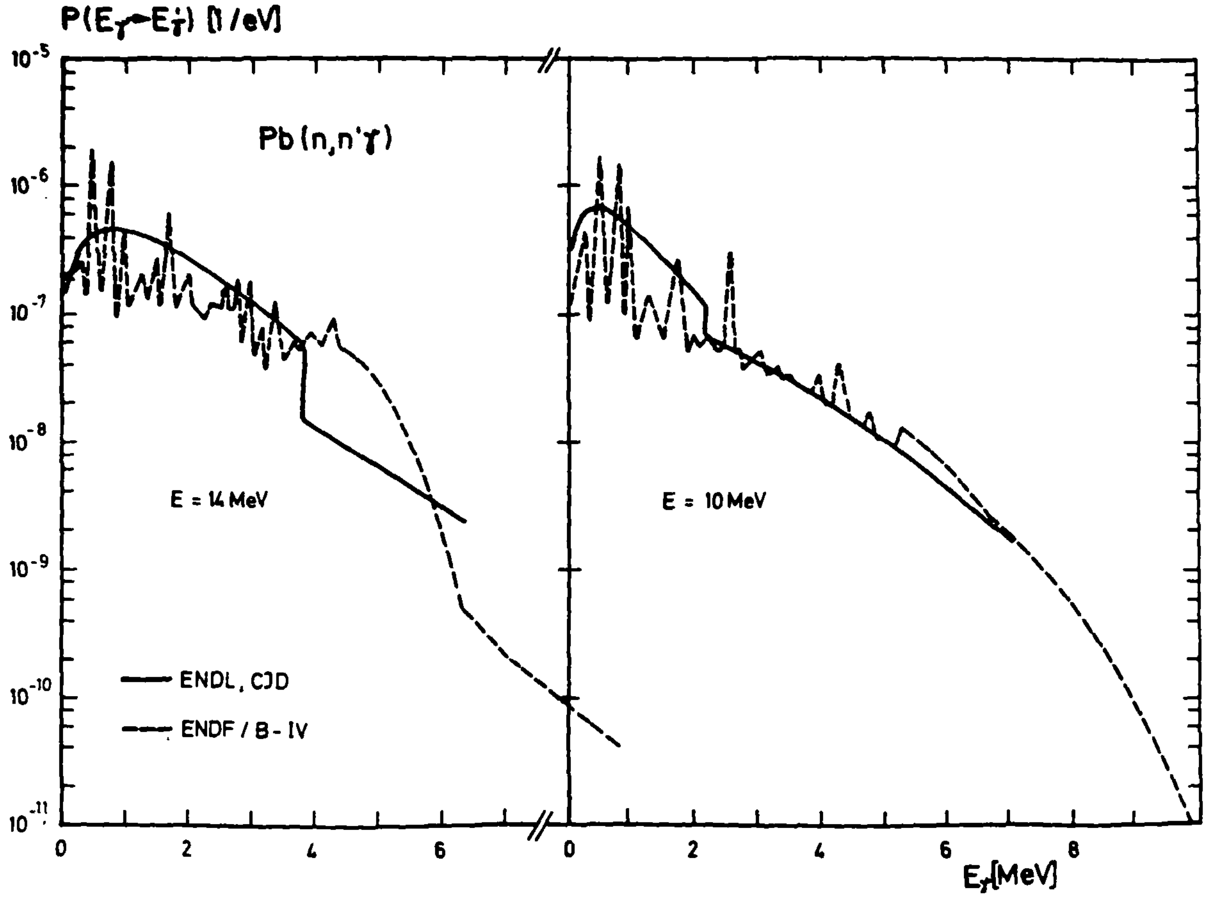

Fig. 33: Neutron-induced γ-ray emission spectra produced by non-elastic processes at 10 and 14 MeV incidence neutrons.

3.3. γ-ray spectra

Analogous to the adoption of ENDL for MF13 the γ-ray emission spectra have been taken from ENDL too.

Basing on the relatively crude R-parameter formalism proposed by Howerton the γ-ray spectra have been estimated (see fig. 33). An investigation performed for Si and Fe /69/ had demonstrated the reasonable reliability of this simple semi-empirical method in prediction of γ-ray spectra.

4. Representation of uncertainties in ENDF/B-format (MF33)

The actual version V of ENDF/B defines also rules and procedures for storage of both the uncertainties of evaluated quantities and their correlations with other data types (covariance matrices).

However, only a few data files (for instance ENDF/B-V Standards Library and the IRDF-versions) have been graduated to provide for such covariance matrices.

MAT 8201 represents a first attempt to test formatting rules.

According to that rules two types of uncertainties have to be distinguished arising from

i) independently evaluated data
and
ii) derived data.

Whereas for the first data typ correlations can only appear between different energy groups of the same type, in the second one correlations between different data quantities have to be taken into considerations.

In MAT 8201 the data types σ_{nT}, $\sigma_{n,n'}$, $\sigma_{n,\gamma}$, $\sigma_{n,\alpha}$, $\sigma_{n,p}$, $\sigma_{n,2n}$, $\sigma_{n,3n}$ have been evaluated independently. Therefore, complementary quantities are treated as correlated with other ones by algebraic equations

Table 16: Relative variances var(σ, σ) /$\sigma \cdot \sigma$ of data evaluated for MAT 8201.

Energy (in eV)	Data types							
	MT1	MT4	MT16	MT17	MT91	MT102	MT103	MT107
1.00-5	0.0	0.0	0.0	0.0	0.0	3.6-3	0.0	0.0
1.00+3	-	-	-	-	-	4.0-2	-	-
1.00+5	2.5-5	-	-	-	-	-	-	-
5.73+5	-	1.0-2	-	-	1.0-2	-	-	-
7.50+5	-	-	-	-	-	-	4.0-2	-
1.00+6	-	4.0-2	-	-	4.0-2	-	-	-
6.76+6	-	-	4.0-2	-	-	-	-	-
7.00+6	-	-	-	-	-	-	-	4.0-2
1.40+7	-	1.0-2	-	-	1.0-2	2.25-2	1.0-2	9.0-2
1.42+7	-	-	-	2.5-1	-	-	-	-
1.50+7	1.0-4	-	2.5-1	-	-	-	-	-
1.70+7	-	4.0-2	-	-	4.0-2	-	-	-
2.00+7	0.0	0.0	0.0	0.0	0.0	0.0	0.0	0.0

$$\sigma_{n,n} = \sigma_{nT} - \sigma_{nX}$$

with

$$\sigma_{nX} = \sigma_{n,n'} + \sigma_{n,\gamma} + \sigma_{n,\alpha} + \sigma_{n,p} + \sigma_{n,2n} + \sigma_{n,3n}.$$

According to this MF33 containes informations on MT1,2,4,10,16,17, 91,102,103,107 directly giving diagonal elements (variances) of the covariances matrices only. The uncertainty $\Delta\sigma$ of a quantity σ at an energy E is defined by the relative variances var $(\sigma,\sigma)\,/\sigma\cdot\sigma$ via the relation

$$\Delta\sigma(E) = \sqrt{\frac{\text{var}\ (\sigma,\sigma)}{\sigma\cdot\sigma}} \cdot \sigma(E) \quad .$$

The uncertainties of any other cross section of the dependent-data type can be determined easily by applying the error propagation rules for the corresponding sum rules given above.

In table 16 all relative variances given in MF33 are compiled.

5. Summary remarks

The actual version of MAT 8201 described in this report tries to fulfill requests arising from different reactor applications (thermal, fast and hybrid reactors).

In comparison with other recent available data files for Lead in the libraries ENDF/B, JENDL and ENDL the most profitable features of MAT 8201 are

i) inclusion of resolved-resonances parameters in MLBW-approach in MF2;
ii) inclusion of energy-angle dependences for neutron inelastic scattering in MF6;
iii) inclusion of γ-ray production cross sections in MF13 and MF15;
iv) inclusion of covariances matrices for important data types in MF33.

Therefore, the present file may be equivalent (or even superior) to the corresponding re-evaluations under development for ENDF/B-VI and EFF-2.

List of references

/1/ D.W. Muir, WRENDA 79/80, INDC(SEC)-73/URSF, 1979

/2/ N. Day Day, WRENDA 81/82, INDC(SEC)-78/URSF, 1981

/3/ V. Piksaikin, WRENDA 83/84, INDC(SEC)-88/URSF, 1983

/4/ H. Gruppelaar, private communication; Neutron Nuclear Data Evaluation Newsletters NNDEN / 34, 1983; NNDEN / 36, 1985

/5/ J. Rapaport, V. Kulkarni, R.W. Finlay, Nucl. Phys. A 330 (1979) 15

/6/ R.W. Finlay, J.R.M. Annand, T.S. Cheema, J. Rapaport, Phys. Rev. C30 (1984) 796
J.R. Annand, R.W. Finlay, F.S. Dietrich, Nucl. Phys. A 443 (1985) 249

/7/ D.E. Bainum, R.W. Finlay, J. Rapaport, J.D. Carlson, Phys. Rev. C16 (1977) 1377

/8/ J. Rapaport, T.S. Cheema, D.E. Bainum, R.W. Finlay, J.D. Carlson, Nucl. Phys. A 296 (1978) 95

/9/ D. Hermsdorf, A. Meister, S. Sassonov, D. Seeliger, K. Seidel, Report ZfK-277(Ü), 1975 and INDC(GDR)-2/L, 1975
D. Hermsdorf, A. Meister, S. Sassonov, D. Seeliger, K. Seidel, Kernenergie 19 (1976) 241

/10/ T. Elfruth, D. Seeliger, K. Seidel, S. Unholzer, in Proc. 13th Int. Symp. on Nuclear Physics, Gaussig, 1983, INDC(GDR)-34/GI, 1985; to be published in Proc. Int. Symp. on Fast Neutron Physics, Chiang Mai, 1985 and Proc. IVth Int. Symp. on Neutron-Induced Reactions, Smolenice, 1985

/11/ A. Takahashi et al., Report OKTAVIAN A-83-01, 1983

/12/ J.L. Kammerdiener, Report UCRL-51232, 1972

/13/ J. Frehaut, G.M. Mosinski, Proc. Int. Symp. on Interaction of Fast Neutrons with Nuclei, Gaussig, 1975, Report ZfK-324, p. 24, 1976
J. Frehaut, A. Bertin, R. Bois, J. Jary, Symp. on Neutron Cross Sections from 10 to 50 MeV, Brookhaven, 1980, Report BNL-NCS-51245, Vol. I, p. 399, 1980

/14/ G. Kießig, Thesis TU Dresden, unpublished, 1975
D. Hermsdorf, G. Kießig, D. Seeliger, Kernenergie 6 (1977) 166

/15/ M. Uhl, B. Strohmaier, Report IRK-76/01, 1976 and addenda to new versions of code STAPRE 1978 and 1981; see also:
M. Uhl, "Nuclear Theory for Application", Trieste, 1982, IAEA-SMR-93, p. 5, 1984

/16/ V.P. Lunev, private communication, 1983

/17/ H. Kalka, D. Hermsdorf, D. Seeliger, A.V. Ignatyuk, V.P. Lunev, Proc. Conf. on Neutron Physics, Kiev, 1983, Vol. I, p. 131, 1984
H. Kalka, D. Hermsdorf, D. Seeliger, Proc. 14th Int. Symp. on Fast Neutron Interaction with Nuclei, Gaussig, 1984, ZfK-562, p. 113, 1985
H. Kalka, D. Hermsdorf, D. Seeliger, Proc. IVth Int. Symp. on Neutron-Induced Reactions, Smolenice, 1985

/18/ V. Benzi et al., Report RT/FI (69) 44, 1969

/19/ E. Běták, J. Dobeš, Phys. Lett. 84B (1979) 368

/20/ A.V. Blokhin, private communication, 1985

/21/ R.B. Schwartz et al., Report NBS-Mono-138, 1974 (data from EXFOR, 1971)

/22/ N. Olsson, B. Holmqvist, E. Ramström, Nucl. Phys. A 385 (1982) 285

/23/ J.P. Delaroche et al., Phys. Rev. C28 (1983) 1410

/24/ M.A. Etemad, Report AE-482, 1973

/25/ B. Holmqvist, T. Wiedling, J. Nucl. Energy 27 (1973) 543

/26/ F.D. Becchetti Jr., G.W. Greenless, Phys. Rev. 182 (1969) 1190

/27/ D. Hermsdorf, Proc. 14th Int. Symp. on Neutron Interaction with Nuclei, Gaussig, 1984, Report ZfK-562, p. 113, 1985

/28/ O. Schwerer, H.D. Lemmel, INDC(NDS)-156, 1984, working paper 25

/29/ ENSDF, Evaluated Nuclear Structure and Decay Data File, Version 1982

/30/ A. Beyerle et al., Proc. Int. Conf. on Nuclear Cross Sections for Technology, Knoxville, 1979, NBS-Special Publication 594, 1984

/31/ D. Hermsdorf. H. Kalka, D. Seeliger, U. Steininger, contribution to "Final Report to CRP on Techniques of Measurements, Analysis and Instrumentation for 14-MeV Neutron Nuclear Cross Sections", IAEA Vienna, to be published, 1986

/32/ R.E. McFarlane, L. Stewart, G. M. Hale, C.L. Dunford, Report LA-UR-84-1026, Revision 1, 1984

/33/ B. Goel et al., Report INDC(GER)-27/LN+Special, 1984

/34/ S. Iwasaki et al., Proc. Symp. Fusion Technology, Jülich, 1982

/35/ Y. Yanagi, A. Takahashi, Report OKTAVIAN A-84-02, 1984

/36/ E.R. Graves, R.W. Davis, Phys. Rev. 97 (1955) 1205

/37/ V.J. Ashby, H.C. Catron, L.L. Newkirk, Phys. Rev. 111 (1958) 616

/38/ P.P. Lebedev et al., Atomn. Ehnerg. 5 (1958) 522, J. Nucl. Energy 11 (1959) 39

/39/ Flerov, N.N., K.M. Talizin, Atomn. Ehnerg. 5 (1958) 657, J. Nucl. Energy 11 (1959) 174

/40/ A. Adam, P. Hrasko, G. Palla, P. Quittner, Nucl. Phys. 49 (1963) 489

/41/ B. Joensson, K. Nyberg, F. Bergqvist, Phys. Scripta 2 (1970) 277, and Ark. Fys. 39 (1969) 295

/42/ Mather et al., Report AWRE-O-47/69, 1969

/43/ G.N. Maslov et al., Yadernije Konstanti 9 (1972) 50 and INDC(CCCP)-49, 1974

/44/ S. Carmona, S. Yiftah, Nucl. Techn. 71 (1985) 289

/45/ M. Segev, M. Caner, Ann. Nucl. Energy 5 (1978) 239

/46/ S. Pearlstein, Nucl. Data Tables A3 (1967) 3

/47/ E. Holub, N. Cindro, J. Phys. G: Nucl. Phys. 2 (1976) 405

/48/ P.E. Vorotnikov, L.S. Larionov, Yad. Fizika 40 (1984) 867

/49/ A.V. Ignatyuk et al., Yad. Fizika 21 (1975) 1185
O.A. Shuravlev et al., Yad. Fizika 26 (1977) 473

/50/ Yu,Ya. Stavisskij et al., Radiatsionnij zakhvat bistrikh nejtronov, Atomizdat, Moskva, 1970

/51/ D.I. Garber, R.R. Kinsey, BNL-325, 3rd edition, Vol. II, 1976

/52/ G.E. Belovitskij, Report ZfK-376, p. 37, 1978

/53/ P. Cuzzocrea, E. Perillo, S. Notarrigo, Nuov. Cimento 4A (1971) 251

/54/ S.M. Qaim, Nucl. Phys. A 185 (1972) 614

/55/ J.A. Holmes, S.E. Woosley, W.A. Fowler, B.R. Zimmerman, Atomic Data and Nucl. Data Tables, 18 (1976) 305

/56/ S.P. Ivanova et al., Yad. Fizika 38 (1983) 1156

/57/ S.M. Qaim, Nucl. Phys. A 382 (1983) 255

/58/ S.M. Qaim, Proc. 3rd Conf. on Neutron Induced Reactions, Smolenice, 1982, in Physics and Applications, Vol. 10, p. 291, 1983

/59/ Z.T. Bödy, K. Mihaly, Report INDC(HUN)-22/L, 1985

/60/ H.L. Taylor, O. Lönsjö, T.W. Bonner, Phys. Rev. 100 (1955) 174

/61/ Yu.G. Degyarev, V.G. Habtochij, At. Ehnerg. 11 (1961) 397

/62/ J.H. Coon et al., Phys. Rev. 111 (1958) 250

/63/ D.G. Foster Jr., D.W. Glasgow, Phys. Rev. C3 (1971) 576

/64/ R.W. Finlay, J.R.M. Annand, J.S. Petler, F.S. Dietrich, Phys. Lett. 155B (1985) 313

/65/ S.F. Mughabghab, Neutron Cross Sections, BNL-325, Vol. I, Part B, Academic Press N.Y., 1985

/66/ D.J. Horen et al., Phys. Rev. C29 (1984) 2126

/67/ G.N. Manturov, V.P. Lunev, L.A. Gorbacheva, Yad. Konst. 52, 1983

/68/ V.M. Dsyuba, L.M. Lazarev, I.N. Paramonova, M.V. Savin, Proc. Neutron Physics Conf., Vol. I, p. 225, Kiev, 1984

/69/ B. Basarragtscha, D. Hermsdorf, D. Seeliger, J. Nucl. Sci. Eng. 83 (1983) 294